Widespread Opportunities for Materials Engineering of Nanocrystals: Advancements towards Synthetically Tailorable Effects and Methodologies

Hayley K. Drozdick,[1,#] Rachel Weiss, [1,#] Colette M. Sullivan, [1,#] Sarah Wieghold[1,2,3] and Lea Nienhaus[1,]*

[1]Department of Chemistry and Biochemistry, Florida State University, Tallahassee, FL 32306, USA

[2]Center for Nanoscale Materials, Argonne National Laboratory, Lemont, IL 60439, USA

[3]Advanced Photon Source, Argonne National Laboratory, Lemont, IL 60439, USA'

*Corresponding Author: lnienhaus@fsu.edu

[#] These authors contributed equally

Abstract

Since their initial development, semiconductor nanocrystals (NCs) and metal nanoparticles (NPs) have become widely utilized in a variety of applications including solar energy harvesting, lighting, catalysis, biomedical imaging, and targeted cancer treatments. Due to their reduced dimensionality, NCs and NPs exhibit vastly different optical and electronic properties than their bulk counterparts, and the properties observed often depend heavily on the NC or NP surface. Surface defects and ligands alter the optoelectronic properties of NCs and NPs and impact their interaction with the environment, allowing for tailoring of their properties without changing the overall chemical composition. In this review, we discuss the research progress focusing on optoelectronic properties of NPs and NCs and their respective applications. Further, we highlight how different surface treatments and ligand functionalization of the particles can influence these applications.

Keywords:

Nanocrystal, nanoparticle, optoelectronic, plasmonic, biological imaging, cancer treatment, catalysis, lighting, ligand chemistry, shells

TOC Graphic

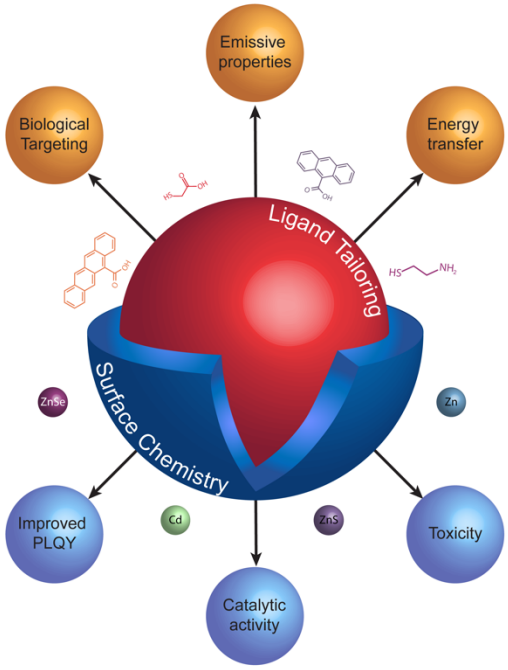

Progress and Potential

The properties of semiconductor nanocrystals (NCs) and metallic nanoparticles (NPs) can be manipulated via surface treatments and ligand functionalization. This enables use in a variety of applications, including solar energy, lighting, displays, catalysis, biological imaging, and targeted cancer treatment. The seminal discoveries discussed in this review are the development of less toxic luminescent NCs, applications of NCs in photon upconversion and the use of NCs as photosensitizers for catalytic applications. Further, we discuss the development of functionalized NPs for biological imaging and as cancer treatments in recent preliminary clinical trials. The potential impact of NCs and NPs is wide reaching and has the potential to improve existing technologies ranging from solar cells and fuel cells to biological imaging and cancer treatments.

1. Introduction

Reducing the dimensionality of materials can result in new optical, electronic, or catalytic properties which make them prime candidates for emerging energy and biomedical applications. In particular, the properties of nanomaterials can be tuned by size, chemical composition, or surface modifications such as ligand functionality and coverage.[1–6] For example, the bandgap of semiconductor nanocrystals (NCs) is largely impacted by their size and dimension of quantum confinement.[7,8] This allows the absorption and photoluminescence (PL) properties of NCs to be altered without changing their underlying chemical composition.[7,9] While conventional spherical NCs, also known as quantum dots (QDs), are confined in all three dimensions, the quantum confinement is relaxed in one direction in elongated nanorods (NRs). Relaxation of the quantum confinement in two dimensions yields nanoplatelets (NPLs), which exhibit quantized bandgaps due to their optical properties being directly dependent on the NPL thickness.[8,10,11] These unique dimensionality-based properties enables the modification of the exciton properties without changing the chemical composition of the NCs. This ease of modification makes NCs appealing for a variety of applications in different fields.[12]

Another important parameter that makes NCs attractive material systems for widespread applications is related to their surface which has the potential to significantly impact the optoelectronic properties. While defects and trap states can decrease the overall PL intensity,[13] targeted surface treatment methods such as shelling can be used to overcome this hurdle.[1,14,15] Additionally, surface ligands of NCs can be easily exchanged to obtain the desired properties, such as end-group functionalization, selective reactivity or increase in stability.[2,16–20] Particularly, ligand binding to the surface can change the electronic properties of a NC, as well as act as a method to prime the NC properties for specific applications.[21,22]

Besides their promising optical properties, NCs are also of interest for catalytic applications.[23–26] The high surface-to-volume ratio of nanoscale catalysts commonly results in higher activity than their bulk counterparts, yielding more cost-effective and sustainable catalytic approaches.[3] The ability to tune the surface ligands of NCs also allows them to be highly versatile, as these can impact the reactivity or modify charge transfer conditions.[3] By further taking advantage of the optical properties of NCs, they can be used to specifically photosensitize catalytic reactions depending on their size.[25]

Similarly, the small size and tunable ligand and surface chemistry of metallic nanoparticles (NPs) enables targeted strategies for biomedical applications.[27–29] For example, NPs can be tuned to absorb in the near infrared (NIR) spectral region which can penetrate deeper into tissue than higher energy light, making them promising contrast agents for biological imaging purposes. By using ligand tailoring, NPs can be used to target individual cells by tuning their affinity to specific biomolecules.[30,31] Moreover, ligands can also be chosen to enable the use of NPs in catalysis. The shape of metallic NPs can be adjusted in order to tune their localized surface plasmon resonances (LSPRs), enabling *e.g.*, field enhancement effects.[32,33]

In this review, we will focus on these tailorable properties of NCs and NPs and discuss the effects of surface-modifications and ligand chemistry on the widespread applications including photon generation and conversion, catalysis, and biomedical applications such as cancer treatment, immunotargeting and biological imaging. An overview of the effects of the surface chemistry is shown in Figure 1. To highlight the breadth of commercial possibilities enabled by NCs and NPs we give several examples for possible applications, rather than an in-depth comprehensive review of each field. For further in-depth reading on the covered topics, we direct the readers to recent

reviews on the surface chemistry of semiconductor NCs,[16,34,35] and the use of NPs for catalysis,[36–38] biological imaging and medicinal applications such as cancer treatments.[39–42]

2. Optoelectronic Applications of NCs: Effect of Surface Treatments

Due to their unique luminescent properties, an application of great interest for semiconductor NCs is in displays, light-emitting diodes (LEDs), and other optoelectronic technologies.[13,43–45] NC LEDs were first developed over 20 years ago,[5] and currently many QD-based displays are commercially available, which show high color purity. The bandgap of NCs, and therefore the emission wavelength, is dependent on the degree of quantum confinement, which can be adjusted by altering the size of the NC relative to the Bohr exciton diameter. Additionally, varying the dimensionality of quantum confinement will affect the absorption properties of the NCs.[46] However, one of the major challenges of NCs and their successful use in optoelectronic applications is related to surface defects. Here, the figure of merit is the PL quantum yield (QY) ϕ: the number of photons emitted by the material with respect to the number of absorbed photons.

NC PL is highly dependent on the surface chemistry of the NCs where surface defects, such as dangling bonds, can act as traps for charge carriers, thus resulting in a decrease of the PLQY.[1] A popular method to increase the PLQY of NCs is the addition of an inorganic semiconductor shell with a wider bandgap than the core NC.[47,48] The inorganic shell serves to passivate the surface trap states, and thus, reduce nonradiative recombination.[1] This process is illustrated in Figure 2A-C. However, depending on the nature of the shell, the addition of an inorganic shell can result in a significant redshift of the absorption and emission wavelengths that increases with shell thickness due to carrier delocalization into the shell material.

Beyond inorganic shells, ligands are required for the colloidal stability of the NCs, as well as provide surface passivation.[49] The surface chemistry of NCs, and therefore the PLQY, can be impacted by ligand electronegativity, vibronic coupling to surface ligands, and compositional changes such as alloying NCs.[1] Another root cause for a decrease in the PLQY in III-V NCs specifically is surface oxidation.[1,47]

Several approaches have been used to overcome the limitations of surface defects based on ligand chemistry, shelling and surface ion addition. In the following, we will discuss the effect of NC surface modifications on their resulting optical properties. For further reading, the reader is directed towards recent reviews on the optoelectronic properties and the relationship to surface chemistry.[1,5,9,16]

2.1. Impact of Ligand Chemistry

Semiconductor NCs require organic ligands for colloidal stability and passivation of surface defects.[49] The chemical nature of the NC ligands directly impacts the resulting optoelectronic properties. For instance, the ligand length, charge, and binding strength to the surface of the NC all influence how a ligand will interact with a NC and impact its stability, optical properties, and capability of undergoing electron transfer processes.[47] In addition, ligand binding to the NC surface is a highly dynamic process which can be tuned by the ligand binding strength: *e.g.*, carboxylic acids are generally loosely bound X-type ligands, while phosphonic acids are strongly bound X-type ligands.[2,50]

In LED applications, obtaining white light emission from luminescent NCs has been an ongoing challenge.[5] The Rosenthal group has been developing and improving white light emitting CdSe NCs since 2005.[44,51–53] In these particles, white light emission is generated by tailoring the

emissive states to cover a broad range of the visible spectrum using methods such as trap emission.[51] Recent work by the Rosenthal group reported record PLQYs of 61.3% for single component white light emitting CdSe NCs after ligand exchange from the native phosphonic acid ligand to citric acid (CA) in a post synthetic treatment.[54] The absorption and emission spectra of these NCs are shown in Figure 3A; the inset demonstrates the visible white light emission of untreated, formic acid treated, and CA-treated NCs.[54] CA treatment was shown to eliminate the size-independent trap state that results from surface passivation by phosphonic acid, allowing size-dependent bandgap emission to take its place. Combining this bandgap emission with selenium surface and deep trap emission features maintained white light emission in CA-treated samples. The stability of the CA-treated NCs was significantly improved compared to previously studied formic acid treated NCs,[55] leading to the conclusion that CA-treated CdSe NCs are a practical option for integration into white light LEDs.

Beyond their application in LEDs, another area of interest for utilizing emissive NCs is as triplet sensitizers in photon upconversion (UC).[8,56–60] UC describes any process where low energy photons are converted into high energy photons, and has potential applications in solar cells, infrared sensing, biological imaging, and photocatalysis.[57,61–64] Here, UC is achieved via triplet-triplet annihilation (TTA), and the unique wavefunction of NCs allows for direct coupling of the excited state to a spin-triplet state in an organic molecule.

However, the long aliphatic ligands required for colloidal stability and high PLQYs of NCs hinder the triplet sensitization performance of the NCs, as they prevent efficient triplet energy transfer from occurring *via* a Dexter-like process, thus leading to low UC QYs.[65] To efficiently funnel the exciton through the ligand shell to the triplet annihilator, the Tang group has pioneered the field of transmitter ligand-enhanced NC-sensitized TTA-UC.[66,67] Overall, improving triplet energy

transfer for CdSe NC sensitizer systems has been achieved to various extents by optimizing the number of bound transmitter ligands, NC size, NC PLQY,[7,68] and by utilizing thin, sub-monolayer shells.[15,69] In 2020, the Tang group achieved near unity efficiency of sensitizer to transmitter ligand TET by using a strongly binding bidentate anthracene diphosphate transmitter ligand, rather than a typical monodentate transmitter ligand, on an unshelled CdSe QD.[70]

In addition to CdSe, PbS and PbSe NCs have been used by the Tang group as triplet sensitizers for NIR-to-visible UC, and addition of transmitter ligands to the NCs is crucial to obtaining efficient UC.[71] Similar to their results using CdSe NCs, it was determined that more quantum confined NCs with well passivated surfaces make better triplet sensitizers, thereby enhancing the UC QY.[72]

The Tang group has recently developed UC systems using silicon NC sensitizers, which would be particularly useful for biological applications due to the relatively nontoxic nature of silicon.[63] They utilized Si NCs that were stabilized *via* a thermal hydrosilylation process as the sensitizer, 9-ethylanthracene (9EA) as the transmitter ligand, and DPA as the emitter. One of the main difficulties in TTA-UC is triplet-scavenging molecular oxygen, which is known to quench the UC yield. However, the thermal hydrosilylation process utilized in this system produced a polymeric barrier to oxygen on the surface of the NC, increasing their oxygen tolerance.[63] The maximum UC QY obtained was reported to be 7.5% out of a maximum of 50% due to the nature of TTA-UC. The Tang group also demonstrated the possibility of UC in water by incorporating this system into micelles with two day air stability and an UC QY of 5.5%, pushing the system towards real-world applications such as biological imaging and photocatalysis.[63]

In addition to semiconducting NCs, metal NPs are a promising materials class for photocatalytic applications and biological imaging due to their lower toxicity and tunable optical properties (*vide infra*). Work by Millstone and coworkers focused on the impact of surface ligands on the PL

properties of Au NPs where NIR emission was induced by exchanging phosphine terminated ligands for sulfur terminated ligands, including thiols and sulfides.[17] The group found that the PLQY varied depending on the identity of the thiol- or sulfide-containing ligand used, with the ligands of the shortest chain-length leading to the greatest PLQY enhancement. They speculated that the substituent group of the ligand could affect both the binding motif of the S-Au bond, as well as the ligand orientation around the gold NPs. Such changes are thought to alter the number of bound ligands, PLQY, and radiative lifetimes depending on which ligands are used on the NP. This work demonstrates the effect of surface chemistry and ligand interaction on PL properties in metal NPs.

2.2. Surface Modification: Surface Ion Addition and Inorganic Shells

In addition to ligand functionalization, applying inorganic shells to the surface of NCs is a common method for controlling surface chemistry of NCs.[47,48] The inorganic shell serves to passivate the surface trap states, and thus, reduce nonradiative recombination.[1] In a type I core/shell structure (Figure 2A), the core NC is surrounded by a wider bandgap material that has both a deeper valence band (VB) and shallower conduction band (CB).[1,48,73] In this configuration, both charges are confined to the core and the exciton bandgap is not drastically influenced. Due to the reduction in quantum confinement caused by shell addition, a small PL redshift is observed, which is dependent on the effective shell thickness.[48] However, in type II or quasi-type II structures, one charge is delocalized into the shell while the other charge remains confined to the core, leading to more significant changes in the PL.[1,48,73]

A reverse type I band structure can also be used in order to confine the electron and hole in the shell of the NC. Dennis and coworkers have reported on a ZnSe/InP/ZnS core/shell/shell with a reverse type I band structure such that the PL properties were dictated by the InP shell thickness,

rather than the ZnSe core diameter.[74] Using this structure, they were able to produce InP-based QDs of various shell thicknesses emitting in the red to NIR regions that are relevant for biological tissue imaging.

While NCs are of great interest for lighting and display technologies, the commonly used CdSe NCs are not encouraged for use in commercial optoelectronic devices due to their toxicity.[75] As a result, less toxic III-V NCs have been developed based on InP for visible light emission. However, as-synthesized InP NCs generally have a PLQY less than 1%, rendering them ineffective for optoelectronic devices. Therefore, the enhancement of the optical properties of InP NCs is of interest to develop viable, nontoxic replacements for Cd- and Pb-based NCs. Electron and hole trapping, as well as surface oxidation are among the most common reasons that InP NCs exhibit such poor optical properties. Surface modification *via* surface addition of ions, shelling, and etching are popular methods for improvement of InP NC PLQYs.[14,47,48,75–77]

One of the common issues found in InP NCs is a natural oxide phase at the NC surface when using traditional fatty acid passivating ligands. This observation has been linked to thermal degradation of the ligands, which in turn results in surface oxidation.[78] To overcome this issue, Jeong and coworkers synthesized tetrahedrally-shaped colloidal InP NCs – the first of their kind – and developed a co-passivation method with chloride ions and primary amines.[78] Importantly, due to the lack of fatty acids used, the authors did not find an oxide signature in their as-synthesized NCs. Following co-passivation, a ZnS shell was added to the NCs and a PLQY of 47% was obtained. Interestingly, the authors found that an oxygen-free environment was required to successfully grow a thick ZnS shell, and that the tetrahedral shape of the InP cores was only maintained in an air-free environment. For many applications, a phase transfer to an aqueous solution is required. The thick shell obtained by this synthetic method yielded very robust particles, as demonstrated by a phase

transfer to basic, aqueous conditions with thioglycolic acid (TGA) as a phase-transferring agent. After a two-hour treatment, the TGA treated core-shell NCs maintained a PLQY of 28%, which amounts to a retention of 60% of the as-synthesized core/shell structure PLQY.

Another option to increase the PLQY of InP NCs is based on the addition of the Lewis acid metals Zn^{2+} and Cd^{2+} to the InP NC surface as demonstrated by Cossairt and coworkers.[79] Surface passivation of dangling bonds by the Lewis acids results in increases in the PLQY from <1% up to 19% and 49% for Zn^{2+} and Cd^{2+}, respectively, without the requirement of a core/shell structure.[79] In addition to the increase in PLQY, redshifts in the emission wavelengths were found, where a higher concentration of Lewis acid yielded a larger shift. This shift is shown in Figure 3B which displays the absorbance spectra of the native InP NCs and Cd^{2+} treated InP NCs.[79] The cause of shifts in optical spectra could not be precisely determined but were hypothesized to result from altering the lowest unoccupied molecular orbital (LUMO) energy level of the NC by the addition of a surface-bound Lewis acid metal cation.

While these described methods serve to improve the PLQY of NCs, color pure NCs are required for commercial applications. While single InP NCs exhibit the required narrow linewidths, obtaining a narrow size distribution is difficult.[80] One of the greatest difficulties in developing a synthesis of more monodisperse InP NCs stems from the generally highly reactive precursors required, *e.g.*, $P(SiMe_3)_3$. Due to the high reactivity, the precursors are generally rapidly depleted in the nucleation phase of NC growth by hot injection. After nucleation, size-narrowing of the NC size distribution is required, which includes unreacted monomers. Side-reactions with the carboxylic acid are also a common occurrence in InP synthesis.[81] As a result, the growth conditions for industrial scale-up of high quality InP NCs have been difficult to obtain. To overcome these limitations, Cossairt and coworkers developed a two-step nucleation mechanism for InP NC

formation with a magic-sized cluster (MSC) intermediate.[80] The MSC intermediates generated at a relatively low injection temperature of 120ºC could be isolated and used as a single-source precursor for subsequent InP NC formation.[82] In a follow-up study, the group investigated the effect of using doped MSCs as precursors for InP NC formation. Zn^{2+} and Ga^{3+} doping, followed by addition of a gradient ZnSeS shell allowed for PLQY up to 85%.[76]

MSCs were also used as precursors in the synthesis of nearly trap free green-emitting InP/ZnSe/ZnS core/shell/shell NCs with 95% PLQY by Jang and coworkers.[77] To demonstrate that this core/shell/shell structure was able to suppress deep trap state emission the authors investigated the temperature-dependence of the InP cores, as well as InP/ZnSe core/shell and InP/ZnSe/ZnS core/shell/shell NCs. Only for the ZnS-terminated core/shell/shell structure, no trap emission is observed at low temperatures, indicative of an effective surface passivation, as shown in Figure 3C.[77]

By combining the described methods of shelling and size control, near-unity PLQY InP NCs can be reliably obtained using methods such as that of Jang and coworkers.[83] The group synthesized InP/ZnSe/ZnS core/shell/shell NCs and performed HF etching to remove the oxide layer on the InP core surface, simultaneous to the start of shell growth.

Since InP NCs with high PLQYs are now routinely attainable, research has progressed into other areas of InP NC improvement in an effort to push towards integration into technology. In most current QD display technologies, the NCs are not utilized in form of true LEDs, but instead function as wavelength downshifters by absorbing blue light and emitting green or red light. However, the change in size of the particles to tune the emission wavelength also influences the absorption cross section of the NCs: larger NCs absorb a higher fraction of the incident blue light. Hence, for display applications, the brightness B_{rel}, defined as the product of the PLQY and

extinction coefficient, must be considered, rather than just the PLQY.[84] Therefore, efforts have been placed on fabricating brightness-matched NCs. The first report of brightness-matched InP/ZnSe/ZnS core/shell/shell NCs was by the Dennis group in 2021.[84] The inherent brightness disparity between different colors of InP NCs was reduced by adjusting the thickness of the intermediate ZnSe shell and InP core such that the total diameter of the InP/ZnSe component was equal among four different emitting colors of NCs. This resulted in brightness matched green and red emitting NCs of the same chemical composition, but different core and inner shell thickness.

In addition to InP NCs, ternary I-III-VI semiconductor NCs such as copper or silver indium selenide have been proposed as non-toxic alternatives to Pb- or Cd-based luminescent NCs in lighting applications.[85,86] In 2013, the Wood group developed a silylamide promoted synthesis with various reaction times and temperatures to control the size and shape of copper indium selenide NCs.[86] Since the native NCs had PLQY around only 15%, the authors added ZnSe shells to increase PLQY to up to 60%. The shells here function similarly to those coating InP NCs as they protect the NC core from degradation induced by oxidation and light exposure and passivate dangling bonds at the surface which can act as nonradiative recombination centers. However, in contrast to the shells discussed previously, where an additional shell is added onto the existing InP core effectively increasing the NC size, the shell growth for the ternary NCs is based on a cation exchange process in which Zn^{2+} replaces the Cu^{+}, Ag^{+} or In^{3+}. Therefore, the shell growth results in slightly smaller overall particle sizes due to the smaller size of Zn^{2+}. In this cation exchange-based shell growth, the shell thickness does not only influence the PLQY, but also shifts the bandgap to higher energies due to increased quantum confinement of the core, as the core is consumed during shell growth.[85,86]

In summary, different methods have been developed to improve the optoelectronic properties of semiconductor NCs to support a transition towards more environmentally or biologically benign materials, which typically exhibit low PLQY without aid. Shelling with different bandgap semiconductors and surface ion addition have been used to improve PLQY,[1,15,48] and a variety of less-toxic NC compositions have been developed to emit at different wavelengths based on their size, surface treatment, and composition.[63,80,83]

3. Catalysis

In addition to their size-dependent optoelectronic properties discussed previously, NCs and NPs also exhibit unique physical properties not found in bulk materials which can make them appealing for applications in catalysis. For instance, as a result of their high surface area to volume ratio, nanoscale catalysts often exhibit higher activity than their bulk counterparts.[3] Due to their optical absorption in the visible range, semiconductor NCs have the additional benefit of being able to engage in photocatalysis, and pose advantages over traditional photocatalysts by acting as both photosensitizer and catalyst in certain reactions.[25] They are also highly stable, and in some cases able to function under conditions unsuitable for traditional bulk catalysts. NCs are also very customizable as the composition, size, and surface modifications of the particle can be altered. Metal NPs are similarly customizable, and bimetallic NPs can pose advantages over traditional catalysis.[36] However, much like in optoelectronic applications control over the surface of NCs and NPs is crucial for effective catalysis.[3,37] The reader is directed to recent reviews on the following reviews on catalysis for further reading.[3,36,38]

3.1. Nanocrystals in Catalysis: Advantages and Limitations

Despite advances in research, NC-based catalysts have drawbacks that must be addressed prior to their successful integration into catalytical schemes. In the case of photocatalysis, the radiative recombination rate is often too fast and the lifetimes too short to properly engage in photocatalysis. For photoredox chemistry, the rates of electron and hole extraction must be balanced to ensure long-term NC stability.[25] As discussed above, ligands pose possibly the largest area of optimization as they can be readily varied, but each change impacts critical properties of the NC such as stability and solubility. While surface ligands are generally considered detrimental to catalysis, if properly designed, they can help increase catalyst selectivity or improve the yield of the desired product.[3] Understanding the interactions between the NC and the surface-bound ligands is crucial for designing NC-based catalysts as ligands can have both steric and electronic effects. As such, the review by Wu and Shevchenko suggests that designing the ligands for surface modification of NCs can improve their performance as photoredox catalysts.[3] Additional work by Weiss and coworkers focusing on PbS NCs adds that the charge density in the ligand shell can be tuned by varying the composition of the ligand shell.[87] This is relevant as the probability of electron exchange is directly related to how permeable the ligand shell is, and thus defines the redox activity of the NC.

Semiconductor NCs have already been implemented as catalysts for multiple reactions such as carbon dioxide reduction, hydrogen evolution reaction (HER), and oxygen reduction reaction (ORR).[26,88,89] CO_2 reduction has applications in several different reactions such as CO and 2-oxoglutarate formation,[24,26] and integrating photocatalysis offers an opportunity to use it for storing solar fuels.

3.2. CO_2 Reduction

Focusing on CO_2 reduction, photocatalytic approaches are particularly appealing to maintain the green nature of this reaction. A system described by Dukovic and coworkers combines CdS NRs

with the enzyme 2-oxoglutarate:ferredoxin oxidoreductase (OGOR) to photochemically produce 2-oxoglutarate by carbon-carbon bond formation *via* CO_2 reduction.[26] Photoexcited electrons from the CdS NRs are transferred to the [4Fe-4S] active site cluster in OGOR where the catalytic process to generate 2-oxoglutarate occurs.. The authors found that the electron transfer efficiency decreases between the CdS NR and enzyme due to the conformational change of OGOR from enzyme-coenzyme coupling.. Nevertheless, their work demonstrates a viable path in which semiconductor NCs, or NRs, can be used as redox partners and electron donors for redox enzymes.

As different semiconductor NCs can be tailored to have similar properties, or even more desirable properties, for different systems, catalyzing CO_2 reduction is not limited to just CdS NCs. For instance, Weiss and coworkers utilized $CuInS_2$/ZnS NCs as a photosensitizer for a molecular catalyst, *meso*-tetraphenylporphyrin iron(III) chloride (FeTPP), for photocatalytic CO_2 reduction.[24] The proposed photocatalytic mechanism is illustrated in Figure 4A.[24] Light generates photoexcited electrons in the NC which in turn transfer to FeTPP reducing the Fe(III) to Fe(0) instigating the reduction of CO_2 to CO. In general, the limitations of molecular sensitization is related to the slow and inefficient electron transfer from the sensitizer to the catalyst. The authors found that the $CuInS_2$/ZnS NC-sensitized system had an 18-fold higher sensitization efficiency than a corresponding system with an Ir-organometallic sensitizer, and exhibited 84% selectivity for CO. This increase in the sensitization efficiency was attributed to an ultrafast electron transfer process between $CuInS_2$ and FeTTP. While still in need of optimization, this system outperformed conventional organometallic-sensitized systems, indicating its high promise.

Further work by Weiss and coworkers investigated the use of an electrostatic assembled superstructure of $CuInS_2$/ZnS NC sensitizers and positively charged trimethylamine-functionalized Fe-porphyrin (FeTMA) catalysts for CO_2 reduction, represented schematically in

Figure 4B.[90] The effect of FeTMA on the optical properties of the NCs is shown in Figure 4C.[90] Reducing CO_2 to CO, their system achieved a turnover number (TON) of 450 and a selectivity of 99%. This was attributed to more efficient funneling of electrons in the charged aggregated superstructure due to the closer proximity of the catalyst and the NCs compared to the uncharged one. This process has been recently improved in another system developed by Weiss and coworkers. Using the same $CuInS_2$/ZnS NCs as photosensitizers and a [{meso-tetra(4-sulfonatophenyl)porphyrinato}cobalt(III)] (CoTPPS) catalyst in pure water, a maximum TON of 84,101 was achieved.[91] This system also illuminated the importance of ligands on catalysis, as the identity of the ligands on $CuInS_2$/ZnS NCs surface had a dramatic impact on catalysis, approximately doubling the TON simply by exchanging the terminal trimethylamine of the aminoethanethiol ligands..

3.3. Hydrogen Evolution Reaction

Research into HER has been similarly successful as CO_2 reduction studies. Many optimizations to NCs have led to achieving successful HER systems. One method of achieving hydrogen evolution is through NC deposition on carbon fiber electrodes. CoP NCs coated electrodes in a system studied by Cossairt and coworkers showed that the impacts of surface ligands change the overpotential of HER.[89] In this study, two ligands motifs that are commonly used in NC synthesis were chosen: carboxylates and amines. A higher ligand density was observed using long carboxylate ligands compared to the amine ones, which was attributed to the stronger binding carboxylate moiety which resulted in an increase in overpotential. This study suggests that the binding strength, *e.g.*, for carboxylates *vs.* amines, influences the ligand density due to stronger/weaker coordination of the moieties which in turn impacts the accessibility to active surface sites for HER.

In a similar method to ligand exchange, NCs themselves can be functionalized to improve their performance. Li and coworkers used a single layer of a metal chalcogenide complex based on tetrathiometallate (MoS_4^{2-} or WS_4^{2-}) which was absorbed onto Au NCs adsorbed onto an activated carbon electrode for the HER.[92] The authors used these self-limiting single monolayer complexes directly as a ligand for the Au NCs which have undergone a colloidal ligand-exchange reaction which is shown schematically in Figure 4D.[92] By comparing two different sizes of Au NCs (9 and 3 nm), the authors found that the Au NC surface had a strong impact on how well the tetrathiometallate, particularly MoS_4, absorbs, packs and oligomerized on the surface.[92] It was shown, that the MoS_x orbitals are strongly hybridized which result in a hydrogen atom bond energy weakening which in turn influences the HER catalytic turnover. Figure 4E-G display the reactivity for HER for the 9 and 3 nm Au@MoS_4 NCs (Figure 4H,I).[92]

As previously discussed, photocatalysis is also possible utilizing NCs, and is also of interest in the HER as it is with CO_2 reduction. A different system described by Weiss and coworkers utilized two NCs rather than one, with one dedicated as a photosensitizer and another as the active catalyst. CdSe/ZnS sensitizer NCs funnel energy into catalytic CdSe/CdS NCs resulting in a photocatalytic reaction and the generation hydrogen from ascorbic acid.[93] The exciton delivery from the sensitizer NC to the catalyst accelerated the sensitization of the catalyst, improving its catalytic activity for the HER.

3.4. Oxygen Reduction Reaction

The oxygen reduction reaction is of interest, as it has been utilized in proton exchange membrane fuel cells.[94] Zhao and coworkers synthesized oxygen-assisted acid etched hollow bimetallic Pt-Ag NPs for use as the catalyst in the ORR.[88] The researchers found that the size and composition can be well controlled for a Pt thickness less than 6 nm which resulted in the desired hollow Pt-Ag

NPs. An overall increase in the ORR activity was observed for these hollow structures compared to the commercial Pt/C, however slight variations were seen for varying NP sizes. The authors speculated that the overall increase in the ORR activity can be attributed to the change in morphology and the addition of Ag into the NPs compared to Pt/C. This work demonstrates a simple design based on hollow bimetallic NPs, which has the potential to be extended to other bimetallic catalysts.

In addition to ligand functionalization and morphology, shelling metal NPs can also be utilized to improve catalytic performance. Research performed by Li and coworkers investigated the influence and thickness of a Pd shell on Au NPs on the ORR. The Au@Pd NPs were synthesized with high control over the number of (sub-)monolayers of the Pd shell utilizing a ligand exchange assisted method. The authors found that the oxide reduction features of PdO shifted depending on the shell thickness.[95] This shift can be directly correlated to Pd surface coverage and the oxygen reduction reactivity. The researchers also predicted that this ligand exchange synthesis would allow other core-shell NPs to tune the electronic properties of the surface, hence improving catalytic activity.

In addition to this study on the impact of size on catalytic performance, Shao-horn and coworkers have also investigated the performance of Pt_3Co NPs for ORR, determining how the addition of Co impacts catalysis.[96,97] One challenge they faced was determining why the performance of these catalytic NPs in cathodes worsened after voltage cycling, as would be seen in a fuel cell.[94] They found that as a result of cycling, the Pt-enriched shell on the NP surface grew thicker, resulting in poorer specific activity as the benefits of Co doping diminished at the surface where catalysis occurs.[94] Pt alloys have improved ORR activity compared to bulk,[96] and by increasing the amount of Pt at the surface relative to Co, this effect would be reduced.

3.5. Photocatalysis and Associated Challenges

In addition to the specific reactions discussed above, semiconducting NCs can also be used to photocatalyze a variety of organic reactions. For instance, McClelland and Weiss utilized CdS NCs as a photocatalyst for the benzyl alcohol oxidation.[98] By tuning the amount of low-valent Cd atoms photodeposited on the NCs, a high selectivity could be achieved for the desired products, *e.g*. benzaldehyde or hydrobenzoin. This system was also able to function without a co-catalyst, simplifying the catalytic process. Further work by Weiss and coworkers showed that CdS NCs can be employed as photosensitizers with a Pd catalyst for the Heck coupling of styrene and iodocyclohexane.[99] This combination indicated that CdS NCs could controllably generate photoexcited states for the Pd catalyst due to an overlap of the CdS emission with the absorption of a Pd(II) intermediate.

NCs can also be used for photoinduced electron transfer reversible addition–fragmentation chain transfer (PET-RAFT) polymerization as demonstrated by Weiss and coworkers.[100] CdSe NCs treated with mercaptopropionic acid (MPA) were used to photocatalyze aqueous acrylamides and acrylates *via* PET-RAFT. The authors showed a fast polymerization with ultralow catalyst loadings. Further emphasis was placed on recycling all the components in the reaction mixture by using a novel purification technique based on protein concentrators.

Despite the promise and versatility of NCs and NPs in catalysis, there are still substantial barriers to practical implementation. The primary challenges facing NC and NP catalysts are the excited state lifetimes, hole extraction, ligand optimization, active sites definition, and reaction conditions optimization.[25] Unfortunately, the excited state lifetimes of NCs can be too short to be useful in photocatalysis. Developing morphological and surface treatments to extend lifetimes and increase PLQYs are then crucial to address this issue.[25,38] Since redox catalysis involves a charge transfer

step, it is important to balance hole and electron extraction to prevent charge buildup which accelerates chemical degradation of the NCs.[25] While the hole extraction rate can be improved by introducing scavenger molecules, there are limits to what can be achieved with this method. More investigation into the active sites is needed to optimize the desired reaction while reducing side reactions, as substrates can bind to the NC surface in multiple modes and geometries. Finally, functionalized NCs are typically soluble in nonpolar solvents, while redox reactions tend to occur in polar solvents. To ensure NC stability, these reactions need to take place in a buffer which maintains pH but does not otherwise interact with the reaction or bind to the NC, causing aggregation or degradation.

Generally, colloidal NCs are promising candidates as photocatalysts due to i) their high absorption range throughout the visible spectrum, ii) tunable absorption and emission, iii) size, which enables ready access to targeted surfaces, and iv) ligand-dependent solubility and functionality which can be changed by the moieties of the ligand.[38] Additionally, semiconductor NCs are desirable as photocatalysts as they are able combine the photosensitizer and catalyst components, thus reducing energy losses in the catalytic process.[25]

4. Cancer Treatments

Another well-studied application of metal NPs is use in targeted cancer treatments.[27,30,41,101,102] Much like semiconductor NCs, the optical properties of plasmonic metal NPs can be controlled by their size, morphology, and surface chemistry.[33] Of particular interest for this application are surface-functionalized gold NPs (AuNPs), due to the biocompatibility and low biotoxicity of gold,[38,42,103] as well as the ability of AuNPs to combine imaging and treatment.[104] For nearly 20 years, these systems have been investigated for targeted tumor therapies.[30,40,105] Light-driven therapies involving NPs pose many advantages over traditional treatments, as they absorb a broad

range of light and emit a narrow spectrum that can be tailored by changing the particle size, composition or by plasmonic tuning of the shell.[30,101,105,106] In particular, a major benefit of plasmonic AuNPs is their optical tunability throughout the NIR spectrum by synthetic methods,[107] enabling deep tissue imaging due to the transparency of water and the transmissivity of biological tissue to these wavelengths.[101,108] By combining these properties, NPs have been implemented in photothermal laser therapies, where a laser is applied to cells treated with NPs which produce heat upon irradiation, resulting in cell death of the cells containing NPs.[27,30,41,109]

The effectiveness of such NP treatments can be seen *in vitro* in Figure 5A, which compares the effect of laser therapy on untreated HER2 positive SKBr3 breast cancer cells, cells treated with NPs without targeting, and cells treated with targeted NPs.[30] The images demonstrate the selectivity and effectiveness of the laser treatment as only the cells with the targeted NPs were destroyed. Figure 5B compares the absorption and scattering efficiency in the NIR spectral region of the NPs used in this study.[30] This early work from 2005 demonstrated the viability of photothermal therapies utilizing NPs, which has been further supported and expanded on by more recent studies. For additional information, the reader is encouraged to read recent reviews on the subject.[29,40,41]

4.1. Progress in Cancer Treatments

Much like in other applications, the unique properties of NPs due to their size and quantum confinement is a part of their appeal in medical applications. The resulting absorption and emission properties of NPs enables their use in both imaging and treatment, as the fluorescence or scattering can be measured *via* different forms of microscopy, while their photothermal properties can be used as a cancer therapy.[101] This specific therapy has the added benefit of being able to target hypoxic regions inside of a tumor which are difficult to access *via* conventional treatment.[101] By

targeting monocytes with NPs which are later recruited into the tumor, these NPs can reach the difficult to target interior of a tumor, increasing the chances of total tumor destruction.[28]

Just as the surface chemistry can impact properties in PL and catalysis, NPs can be functionalized to improve their therapeutic and imaging performance. NPs can be functionalized to interact with specific biomolecules such as proteins or antibodies present in tumors, therefore allowing for highly specific targeting of tumors where these biomolecules are found in abundance. Due to their combined diagnostic and therapeutic applications, functionalized metal NPs are often classified as theragnostic materials.[110] A review by Murphy and coworkers focusing on nanotechnology based treatments of breast cancer examined a variety of organic and inorganic NPs for different applications within cancer therapeutics.[41] They found that despite the promise of these materials for cancer treatments, unresolved concerns over toxicity, biocompatibility and molecular display need to be addressed prior to implementation. With proper surface functionalization NPs can engage in active targeting of tumor cells, while current treatments primarily use passive targeting. Beyond cancer treatment, functionalized NPs show promise in the areas of gene therapy, targeted drug delivery, and imaging (*vide infra*).[41]

Functionalized AuNPs have been successfully used to treat different forms of cancer, such as breast cancer, in both *in vitro* and *in vivo* animal studies.[40,105,111] Functionalized NPs are of particular interest for difficult to treat forms of cancer, as their active targeting and ability to reach areas inaccessible *via* conventional therapies provide routes to address some of the shortfalls of traditional therapies.[28] Targeting these areas not only allows for better treatment of the tumor itself, but could also prevent metastatic spread by treating the tumor more comprehensively.

Having proven effective in vitro and in vivo, NP-based cancer treatments are beginning to move beyond the stage of animal studies. A recent clinical study using NP accumulation in tumors

combined with infrared (IR) irradiation to treat prostate cancer had very promising results, with a 94% success rate of laser ablation.[27] This treatment was shown to both reduce side effects and be less invasive than other treatment options for this form of cancer. These promising results pave a pathway towards larger clinical trials, and possibly show potential for widespread cancer treatments in the near future.

4.2. Challenges in Advancing NP-based Cancer Therapy

Despite their incredible promise for cancer treatments, there are still some unresolved concerns about the impact of NPs on the human body that must be addressed prior to widespread medical applications.[42] While AuNPs are generally considered to be nontoxic,[103] this does not preclude them from having a negative impact on the cells they contact. In particular, the NR morphology has been shown to damage the collagen extracellular matrix.[108] Grzincic and Murphy found that this damage can result in lower adhesion of the cells to the collagen matrix, which can in turn promote cell spread. This is particularly dangerous when dealing with cancerous cells, as the spread of cancerous cells could worsen the illness rather than treat it. While this effect, examined mostly in *in vitro* studies, varies depending on the morphology of the AuNP and their surface functionalization, it is an important concern to have addressed prior to clinical application.[108,112] This is not the only impact NPs can have on cells without being directly toxic. Murphy and coworkers reported that functionalized NPs interfere with chemotaxis, cell movement in response to a chemical.[112] AuNPs were found to impact the bioavailability of a chemoattractant biomolecule MCP-1, since this molecule adsorbs to the NP surface. Higher quantities of MCP-1 absorption onto the NP surface resulted in stronger suppression of cell movement. Therefore, the NP-based treatment could result in an unintentional impact on the movement of cancer cells, and more

research will be required to determine the underlying causes and how to limit this effect prior to its widespread application.

5. Biological Imaging

In addition to applications in cancer treatments, NPs have been used for other forms of biological imaging.[102,113,114] The same properties that make NPs beneficial for cancer treatment, *e.g.*, IR absorption[30,107,115] and surface functionalization for targeting biomolecules,[41,116] make them well suited for biological imaging, where these properties can be used to image specific cells or even cellular processes. NPs can be used as contrast agents,[104,117–120] for light-triggered applications,[110,121–125] and for immunotargeted imaging.[29,116,126]

5.1. NPs as Contrast Agents for Biological Imaging

One of the primary applications of NPs in cellular imaging is as a contrast agent. Murphy and coworkers used relaxation imaging measurements to demonstrate how strongly absorbing gold NRs (AuNRs) affect protein binding and protein folding accounting for inner filter effects, including the strong quenching effect of AuNRs on fluorescent protiens.[117] The high absorbance of NRs is desirable for sensitive detection but also makes optical experiments more difficult as it can result in unwanted quenching of fluorescent-tagged proteins. This work demonstrated the use of two photon photoluminescence of AuNRs to image the NRs in tissue constructs, showing the viability of AuNRs as a contrast agent in optical coherence microscopy. By using optical coherence microscopy (OCL) and two photon luminescence (TPL) on cells with and without NRs, the positioning of the Au NRs inside the cell were imaged. Fluorescence imaging was also used to measure the impact of NRs on proteins, as fluorescently tagged proteins were combined with Au NRs and imaged using fluorescence microscopy.[117]

Focusing on specific applications in studying cellular processes and developing intracellular targeted therapies, Halas and coworkers demonstrated that light-triggered release of the fluorescent dye 4′,6-diamidino-2-phenylindole (DAPI) from plasmonic gold nanoshells was feasible and did not damage cells.[121] This is a potential method of delivery for gene therapy, as the DAPI was taken into the cell nucleus and was able to bind to genomic DNA. Other molecules which bind to DNA could be used in such a manner.

Beyond biological cell imaging contrasts, NPs also have applications as magnetic resonance imaging (MRI) contrast agents.[127] The Millstone group has utilized metal alloys to improve optical properties of NIR emitting gold NPs, which could potentially be used for biological sensing and labeling.[17,118,119] They obtained bright NIR emission *via* alloying gold with cobalt or copper on the nanoscale for the first time. Notably, alloying with cobalt resulted in tunable magnetic susceptibility of the gold NPs, opening up the possibility for gold NPs to be used as MRI contrast agents.[118] The emission peaks blueshift as the amount of incorporated cobalt increases to 60%, then have a slight redshift up to 80% cobalt. The impact of Co doping on magnetic properties is similar, as the magnetic susceptibility increases with percent Co. The Millstone group was also the first to demonstrate NIR emission from copper and silver NPs, which could serve as a cost-efficient alternative to gold NPs in biomedical applications.[128] The Ag and Cu NPs developed exhibited comparable brightness and QY to AuNPs, but their applicability in biological system has been less studied than AuNPs. Future research is necessary in order to improve QYs of NIR emitters, especially at low excitation wavelengths, develop a better understanding of coinage metal (Cu, Ag, Au) NP surfaces, and better understand how Ag and Cu perform in the place of Au in biological applications.[128,129]

5.2. Cell Imaging

In addition to applications as contrast agents, NPs can also be utilized as an aid in cell imaging techniques. Early work in 2007 demonstrated that AuNRs could be used to image deformation in collagen matrixes as a result of cell motion.[130] This work displayed the viability of this technique, and used it to improve understanding of the collagen matrix. Baxter and coworkers expanded on this work, describing how the light scattering properties of various morphologies of AuNPs made it possible to track the position of individual NPs, as well as how the morphology of AuNPs can be tailored to the desired imaging wavelength as NRs absorb more into the NIR-vis region than nanospheres.[115] Major advantages of AuNRs are that they do not photobleach and can be nontoxic, both of which make them a promising alternative to traditional dyes.

Even in this early work, toxicity of metal NPs was a focus of research. Baxter and coworkers determined no direct NP cytotoxicity, but indicated that the NP precursors were toxic at very low concentration, emphasizing the need for purification of the NPs.[115] The authors found cytotoxicity to be cell and surface chemistry dependent as different cells interact with NPs in different ways, and emphasized toxicity is not equivalent to cellular damage, as 13 nm citrate capped gold nanospheres resulted in cellular damage but were not considered toxic. However, AuNPs treated with other surface treatments were shown to be toxic to the studied cells. Figure 6A,B show the relationship between the AuNPs and cells via dark-field optical microscopy (Figure 6A) and fluorescent staining (Figure 6B).[115] It was also established that the uptake of polyethylene glycol (PEG) coated AuNRs was significantly lower than regularly functionalized counterparts.

As discussed above, another benefit of NP imaging is that they can be functionalized to target specific cells or biomolecules.[29] The ability to track single NPs can be used to track individual proteins in extra and intracellular regions. NP surface passivation also enables colloidally stable

small NPs, which could be used to image regions like synapses that are difficult to image by other means.

5.3. Immunotargeting

This surface functionalization leads to another area of particular interest in cellular imaging, immunotargeting using NPs, which holds great potential for both diagnostic and research purposes.[126] The ability to target specific biomolecules could allow for targeting of specific cellular processes of interest. Research focused on sulfated glycosaminoglycans (sGAG) functionalized AuNRs examined the interaction between the NR and cardiac cells and collagen, establishing that surface modification with biological polyanions can improve their viability in biological or therapeutic applications.[131] However, it was found that functionalizing the AuNRs increased the amount of collagen aggregation in a collagen gel assay and created a stiffer collagen structure than a control, although the exact mechanics were unclear. The surface functionalization appeared to incorporate the NRs within the aggregates, suggesting a strong interaction between the sGAG and collagen, altered by the NR binding. The functionalized NRs accelerated assembly of collagen cells and inhibited cell mediated contraction without impacting cell viability, which could result in reducing accumulation of scar tissue and promoting regeneration of functional tissue.

Murphy and coworkers continued to investigate immunotargeted AuNRs, specifically focusing on how ligand-functionalized AuNRs can be used to control interactions with cancer cells.[132] A schematic of how the AuNRs were modified is shown in Figure 6C, and the peptide arrangement on the surface is illustrated in Figure 6D,E.[132] Comparing AuNRs functionalized to target specific cancer cells, they demonstrated that these NRs successfully targeted the desired cells over a control. They were also able to use homing peptides with AuNRs to quantify the uptake of NRs inside cells, which provides a pathway to evaluate the specificity of ligands for targeted drug

delivery systems based on functionalized AuNRs. This is demonstrated in transmission electron microscopy images shown in Figure 6F-K, where the different ligands are shown to remain in the cells in different quantities over time.[132]

Combining the imaging and immunotargeting aspects of NCs, research from Rosenthal and coworkers used functionalized NCs to image a dopamine transmitter (DAT) which has been associated with schizophrenia, bipolar disorder, Parkinson's and attention-deficit hyperactivity disorder.[116] Commercially available Streptavidin conjugated CdSe/ZnS core/shell NCs were used for this purpose. It had been difficult to image DAT using conventional methods due to the difficulty in finding a photostable targeted molecule. The accuracy, brightness, and resistance to photodegradation of NCs posed a solution to these problems, enabling effective imaging. The broad absorption of NCs paired with sharp emission also simplified molecular imaging. The results of this experiment demonstrated the specificity of the functionalized NCs and their high sensitivity and posed the advantages over conventional imaging approaches for this protein.

5.4. Challenges in Biological Imaging using NCs

Metal NP-based imaging faces challenges due to size, multivalent interactions with biomolecules, and blinking.[29] A smaller size is generally desirable for *in vivo* applications, as it allows for finer resolution and imaging with high spatial resolution, and NPs over a certain diameter are more difficult to clear from the body. However, smaller NPs could perform better as certain therapeutics, but can pose a particular danger as they can disrupt cell membranes and are generally more toxic than their larger counterparts, while large NPs exhibit more efficient absorption and scattering, which is beneficial for theranostic applications.[109] In addition, small NPs can become catalytically active and thus, induce additional cytotoxicity.[133]

Focusing on one potential problem, multivalency could result in undesired conjugation of multiple copies of biomolecules to the NP, which in turn could result in protein crosslinking, activation of signaling pathways, impairment of surface protein mobility, or even an increase the cytotoxicity of multivalent NP conjugates. However, some applications such as drug carriers or imaging agents may benefit from using multivalent NPs. Blinking can make it harder to track individual NPs in time lapse image sequence, but as a contrast can also help distinguish single NPs from aggregates.

While Au NPs are generally considered nontoxic, the use of certain ligands can make them toxic and some ligands are toxic on their own, such as the commonly used cetyltrimethylammonium bromide (CTAB), meaning any NPs using these ligands would need to be highly purified and studied prior to use in biological applications to ensure their safety.[31,42,134]

Despite their classification as non-cytotoxic, exposure to NPs can result in long term changes to human cells. Murphy and co-workers compared the effects of a variety of different AuNPs of different sizes, morphologies, and surface coatings on human dermal fibroblasts (HDF).[133] Comparing the effects of chronic and nonchronic low dose exposure to AuNPs, both resulted in modification to genes over time but the nonchronic exposure resulted in more changes than the chronic exposure, showing stress effects even 20 weeks after initial exposure. The authors suggest that cells can respond and learn to adapt to chronic NP exposure, but even after the removal of NPs in acute exposure, the cell stress response was not reversible. Low doses of AuNPs that initially appeared benign were shown to destabilize cell regulatory responses over time. In general, it was found that AuNPs are not directly cytotoxic and relative uptake is dependent slightly on the shape and more heavily on surface coating, but over time AuNPs in some cases were shown to cause changes to the morphology and gene expression of the cell.

Additional work by Murphy and coworkers found that coated AuNPs can affect genes including those implicated in cell proliferation and metabolism in HDF and prostate cancer (PC3) cells.[136] This work focused on showing the connection between surface coating and toxicity in different cells depending on factors including ligand binding strength, electrostatic NP-protein interactions, and uptake rate. Some surface treatments had no significant impact on the cell, while others resulted in up-regulation of cell genes which could lead to tumor development. The effects differed as a result of not only NP surface chemistry, but also on NP dosage and which cell type was exposed. While still considered generally nontoxic, the changes caused by AuNPs are still a cause concern for future medical applications.

Another concern in using metal NPs or semiconductor NCs for biological applications is the difference in quality in the commercially available materials and those typically used for research purposes. This could potentially have harmful effects, as some NC precursors are highly toxic, and even nontoxic interactions between the NCs and cells could result in detrimental changes to the cell environment. Recent work by Han and coworkers focused on establishing an understanding of how different synthetic parameters could be altered to overcome this disparity in NC quality.[137] Specifically, they determined that growth temperature and precursor reactivity were the most important factors for controlling NC quality, and controlled this using a sulfur precursor with a chemically tunable reactivity. Using this precursor, they were able to demonstrate the viability of the described method for a variety of sizes, materials, and types of NCs.

6. Conclusion

Semiconductor NCs and (plasmonic) metal NPs are a versatile class of materials as their properties are highly tunable *via* surface treatments and ligand chemistry. The properties of NCs can be altered by changing the chemical composition or by varying the morphology of NCs within the

same composition.[7,8,68,99] The optical properties of NCs are largely controlled by their size and shape, and as a result, large NCs will absorb and emit different wavelengths than smaller NCs.[4,68,86] The degree of quantum confinement also plays a significant role, as NC properties differ from those of NRs which differ from NPLs.[8,68] Surface treatments such as shelling or ion exchange can also be used to further control the properties of a NC. Utilizing shells with a different composition than the NC core can reduce nonradiative decay for optoelectronic applications by defect passivation and improve QY at the cost of a shift in the emission wavelength[14,15,48,62] and ion exchange can further passivate surface defects.[78,79] While less optically active, metal NPs can be similarly treated via ligand functionalization or ion exchange to tailor their properties toward a specific application or system.

Ligand chemistry potentially holds the broadest area of variability for NCs as ligand chemistry can tailor the NC properties for specific applications.[2,17,18,70,116] For catalysis, ligand chemistry can be used to convert NCs into efficient photosensitizers, allowing conventional catalytic reactions to become photocatalytic.[25,90] For biological applications, ligand chemistry can be used to target NPs to specific types of cells for better treatment or imaging.[27,30,41,101] Ligand chemistry is incredibly important for these applications, as it will significantly alter how NPs interact with cells and how harmful, if at all, those interactions are.[31,136] However, surface ligands can also induce toxicity, as some ligands are themselves toxic.[31,42,134]

Overall, the largest challenge facing NC or NP implementation is the ongoing issue of toxicity. Many high-performance NCs utilize heavy metals, which pose both health and environmental concerns.[69,70,87,99] While efforts have been made to replace these heavy metals with less toxic or benign alternatives such as InP and silicon,[63,81,83] NCs themselves are often toxic simply by the nature of their size. The size of NPs enables them to interact with cells in unique ways, which are

not always desirable. Even if the NPs used are not toxic, they can still cause damage to cells that can result in long-term changes to the cell's overall health.[131,133]

In summary, semiconductor NCs and metal NPs have the potential to dramatically alter many aspects of our lives, from optical applications in everyday devices to catalysis which could alter fuel production, to medical treatments that could improve how we research different diseases and treat cancer.[5] The field is now reaching the point where this potential is beginning to come to fruition. While there is still a significant amount of research needed for most NC and NP applications, future developments in the field are likely to realize more extensive implementation of these nanoscale materials throughout society.

Acknowledgements

The authors acknowledge Florida State University for funding. Work performed at the Center for Nanoscale Materials and Advanced Photon Source, both U.S. Department of Energy Office of Science User Facilities, was supported by the U.S. DOE, Office of Basic Energy Sciences, under Contract No. DE-AC02-06CH11357.

Author Information

Corresponding Author:

*Lea Nienhaus: nienhaus@chem.fsu.edu

Author contributions

H.D.K, R.W. and C.M.S. contributed equally. Conceptualization: L.N.; All authors contributed

to the writing of the manuscript.

ORCID

Sarah Wieghold: 0000-0001-6169-3961

Lea Nienhaus: 0000-0003-1412-412X

Declaration of Interests

L.N. is a member of the editorial advisory board of Matter.

REFERENCES

1. Eagle, F.W., Park, N., Cash, M., and Cossairt, B.M. (2021). Surface Chemistry and Quantum Dot Luminescence: Shell Growth, Atomistic Modification, and Beyond. ACS Energy Lett. *6*, 977–984.

2. Huang, Z., and Tang, M.L. (2017). Designing Transmitter Ligands That Mediate Energy Transfer between Semiconductor Nanocrystals and Molecules. J. Am. Chem. Soc. *139*, 9412–9418.

3. Wu, W., and Shevchenko, E.V. (2018). The surface science of nanoparticles for catalysis: electronic and steric effects of organic ligands. J. Nanoparticle Res. *20*, 255.

4. Swafford, L.A., Weigand, L.A., Bowers, M.J., McBride, J.R., Rapaport, J.L., Watt, T.L., Dixit, S.K., Feldman, L.C., and Rosenthal, S.J. (2006). Homogeneously Alloyed CdSxSe1-x Nanocrystals: Synthesis, Characterization, and Composition/Size-Dependent Band Gap. J. Am. Chem. Soc. *128*, 12299–12306.

5. Frecker, T., Bailey, D., Arzeta-Ferrer, X., McBride, J., and Rosenthal, S.J. (2015). Review—Quantum Dots and Their Application in Lighting, Displays, and Biology. ECS J. Solid State Sci. Technol. *5*, R3019.

6. VanOrman, Z.A., and Nienhaus, L. (2021). Recent advancements in halide perovskite nanomaterials and their optoelectronic applications. InfoMat *3*, 962–986.

7. Rigsby, E.M., Miyashita, T., Jaimes, P., Fishman, D.A., and Tang, M.L. (2020). On the size-dependence of CdSe nanocrystals for photon upconversion with anthracene. J. Chem. Phys. *153*, 114702.

8. VanOrman, Z.A., Bieber, A.S., Wieghold, S., and Nienhaus, L. (2020). Green-to-Blue Triplet Fusion Upconversion Sensitized by Anisotropic CdSe Nanoplatelets. Chem. Mater. *32*, 4734–4742.

9. Chern, M., Kays, J.C., Bhuckory, S., and Dennis, A.M. (2019). Sensing with photoluminescent semiconductor quantum dots. Methods Appl. Fluoresc. *7*, 012005.

10. Vong, A.F., Irgen-Gioro, S., Wu, Y., and Weiss, E.A. (2021). Origin of Low Temperature Trion Emission in CdSe Nanoplatelets. Nano Lett. *21*, 10040–10046.

11. Dufour, M., Qu, J., Greboval, C., Méthivier, C., Lhuillier, E., and Ithurria, S. (2019). Halide Ligands To Release Strain in Cadmium Chalcogenide Nanoplatelets and Achieve High Brightness. ACS Nano *13*, 5326–5334.

12. Lohse, S.E., and Murphy, C.J. (2012). Applications of Colloidal Inorganic Nanoparticles: From Medicine to Energy. J. Am. Chem. Soc. *134*, 15607–15620.

13. Jang, E., Kim, Y., Won, Y.-H., Jang, H., and Choi, S.-M. (2020). Environmentally Friendly InP-Based Quantum Dots for Efficient Wide Color Gamut Displays. ACS Energy Lett. *5*, 1316–1327.

14. Mundy, M.E., Eagle, F.W., Hughes, K.E., Gamelin, D.R., and Cossairt, B.M. (2020). Synthesis and Spectroscopy of Emissive, Surface-Modified, Copper-Doped Indium Phosphide Nanocrystals. ACS Mater. Lett. *2*, 576–581.

15. Huang, Z., Xia, P., Megerdich, N., Fishman, D.A., Vullev, V.I., and Tang, M.L. (2018). ZnS Shells Enhance Triplet Energy Transfer from CdSe Nanocrystals for Photon Upconversion. ACS Photonics *5*, 3089–3096.

16. Morris-Cohen, A.J., Malicki, M., Peterson, M.D., Slavin, J.W.J., and Weiss, E.A. (2013). Chemical, Structural, and Quantitative Analysis of the Ligand Shells of Colloidal Quantum Dots. Chem. Mater. *25*, 1155–1165.

17. Crawford, S.E., Andolina, C.M., Smith, A.M., Marbella, L.E., Johnston, K.A., Straney, P.J., Hartmann, M.J., and Millstone, J.E. (2015). Ligand-Mediated “Turn On,” High Quantum Yield Near-Infrared Emission in Small Gold Nanoparticles. J. Am. Chem. Soc. *137*, 14423–14429.

18. Ritchhart, A., and Cossairt, B.M. (2019). Quantifying Ligand Exchange on InP Using an Atomically Precise Cluster Platform. Inorg. Chem. *58*, 2840–2847.

19. Morris-Cohen, A.J., Donakowski, M.D., Knowles, K.E., and Weiss, E.A. (2010). The Effect of a Common Purification Procedure on the Chemical Composition of the Surfaces of CdSe Quantum Dots Synthesized with Trioctylphosphine Oxide. J. Phys. Chem. C *114*, 897–906.

20. McArthur, E.A., Godbe, J.M., Tice, D.B., and Weiss, E.A. (2012). A Study of the Binding of Cyanine Dyes to Colloidal Quantum Dots Using Spectral Signatures of Dye Aggregation. J. Phys. Chem. C *116*, 6136–6142.

21. Knowles, K.E., Tice, D.B., McArthur, E.A., Solomon, G.C., and Weiss, E.A. (2010). Chemical Control of the Photoluminescence of CdSe Quantum Dot−Organic Complexes with a Series of Para-Substituted Aniline Ligands. J. Am. Chem. Soc. *132*, 1041–1050.

22. Knowles, K.E., Frederick, M.T., Tice, D.B., Morris-Cohen, A.J., and Weiss, E.A. (2012). Colloidal Quantum Dots: Think Outside the (Particle-in-a-)Box. J. Phys. Chem. Lett. *3*, 18–26.

23. Gou, L., and J. Murphy, C. (2005). Rod-like Cu/La/O nanoparticles as a catalyst for phenol hydroxylation. Chem. Commun. *0*, 5907–5909.

24. Lian, S., Kodaimati, M.S., Dolzhnikov, D.S., Calzada, R., and Weiss, E.A. (2017). Powering a CO2 Reduction Catalyst with Visible Light through Multiple Sub-picosecond Electron Transfers from a Quantum Dot. J. Am. Chem. Soc. *139*, 8931–8938.

25. Kodaimati, M.S., McClelland, K.P., He, C., Lian, S., Jiang, Y., Zhang, Z., and Weiss, E.A. (2018). Viewpoint: Challenges in Colloidal Photocatalysis and Some Strategies for Addressing Them. Inorg. Chem. *57*, 3659–3670.

26. Hamby, H., Li, B., Shinopoulos, K.E., Keller, H.R., Elliott, S.J., and Dukovic, G. (2020). Light-driven carbon−carbon bond formation via CO2 reduction catalyzed by complexes of CdS nanorods and a 2-oxoacid oxidoreductase. Proc. Natl. Acad. Sci. *117*, 135–140.

27. Rastinehad, A.R., Anastos, H., Wajswol, E., Winoker, J.S., Sfakianos, J.P., Doppalapudi, S.K., Carrick, M.R., Knauer, C.J., Taouli, B., Lewis, S.C., et al. (2019). Gold nanoshell-localized photothermal ablation of prostate tumors in a clinical pilot device study. Proc. Natl. Acad. Sci. *116*, 18590–18596.

28. Choi, M.-R., Stanton-Maxey, K.J., Stanley, J.K., Levin, C.S., Bardhan, R., Akin, D., Badve, S., Sturgis, J., Robinson, J.P., Bashir, R., et al. (2007). A Cellular Trojan Horse for Delivery of Therapeutic Nanoparticles into Tumors. Nano Lett. *7*, 3759–3765.

29. Rosenthal, S.J., Chang, J.C., Kovtun, O., McBride, J.R., and Tomlinson, I.D. (2011). Biocompatible Quantum Dots for Biological Applications. Chem. Biol. *18*, 10–24.

30. Loo, C., Lowery, A., Halas, N., West, J., and Drezek, R. (2005). Immunotargeted Nanoshells for Integrated Cancer Imaging and Therapy. Nano Lett. *5*, 709–711.

31. Burrows, N.D., Lin, W., Hinman, J.G., Dennison, J.M., Vartanian, A.M., Abadeer, N.S., Grzincic, E.M., Jacob, L.M., Li, J., and Murphy, C.J. (2016). Surface Chemistry of Gold Nanorods. Langmuir *32*, 9905–9921.

32. Murphy, C.J., Gole, A.M., Hunyadi, S.E., Stone, J.W., Sisco, P.N., Alkilany, A., Kinard, B.E., and Hankins, P. (2008). Chemical sensing and imaging with metallic nanorods. Chem. Commun., 544–557.

33. Cai, Y.-Y., Choi, Y.C., and Kagan, C.R. Chemical and Physical Properties of Photonic Noble-Metal Nanomaterials. Adv. Mater. *n/a*, 2108104.

34. Cossairt, B.M. (2016). Shining Light on Indium Phosphide Quantum Dots: Understanding the Interplay among Precursor Conversion, Nucleation, and Growth. Chem. Mater. *28*, 7181–7189.

35. Eagle, F.W., Rivera-Maldonado, R.A., and Cossairt, B.M. (2021). Surface Chemistry of Metal Phosphide Nanocrystals. Annu. Rev. Mater. Res. *51*, 541–564.

36. Sytwu, K., Vadai, M., and Dionne, J.A. (2019). Bimetallic nanostructures: combining plasmonic and catalytic metals for photocatalysis. Adv. Phys. X *4*, 1619480.

37. Weiss, E.A. (2017). Designing the Surfaces of Semiconductor Quantum Dots for Colloidal Photocatalysis. ACS Energy Lett. *2*, 1005–1013.

38. Wilker, M.B., Schnitzenbaumer, K.J., and Dukovic, G. (2012). Recent Progress in Photocatalysis Mediated by Colloidal II-VI Nanocrystals. Isr. J. Chem. *52*, 1002–1015.

39. Alkilany, A.M., Thompson, L.B., Boulos, S.P., Sisco, P.N., and Murphy, C.J. (2012). Gold nanorods: Their potential for photothermal therapeutics and drug delivery, tempered by the complexity of their biological interactions. Biol. Interact. Nanoparticles *64*, 190–199.

40. Abadeer, N.S., and Murphy, C.J. (2016). Recent Progress in Cancer Thermal Therapy Using Gold Nanoparticles. J. Phys. Chem. C *120*, 4691–4716.

41. Falagan-Lotsch, P., Grzincic, E.M., and Murphy, C.J. (2017). New Advances in Nanotechnology-Based Diagnosis and Therapeutics for Breast Cancer: An Assessment of Active-Targeting Inorganic Nanoplatforms. Bioconjug. Chem. *28*, 135–152.

42. Alkilany, A.M., and Murphy, C.J. (2010). Toxicity and cellular uptake of gold nanoparticles: what we have learned so far? J. Nanoparticle Res. *12*, 2313–2333.

43. Kim, T., Kim, K.-H., Kim, S., Choi, S.-M., Jang, H., Seo, H.-K., Lee, H., Chung, D.-Y., and Jang, E. (2020). Efficient and stable blue quantum dot light-emitting diode. Nature *586*, 385–389.

44. Schreuder, M.A., Xiao, K., Ivanov, I.N., Weiss, S.M., and Rosenthal, S.J. (2010). White Light-Emitting Diodes Based on Ultrasmall CdSe Nanocrystal Electroluminescence. Nano Lett. *10*, 573–576.

45. Kim, K., Han, C.-S., and Jeong, S. (2012). Design and synthesis of photostable multi-shell Cd-free nanocrystal quantum dots for LED applications. J. Mater. Chem. *22*, 21370–21372.

46. VanOrman, Z.A., Bieber, A.S., Wieghold, S., and Nienhaus, L. (2020). Green-to-Blue Triplet Fusion Upconversion Sensitized by Anisotropic CdSe Nanoplatelets. Chem. Mater. *32*, 4734–4742.

47. Kim, Y., Chang, J.H., Choi, H., Kim, Y.-H., Bae, W.K., and Jeong, S. (2020). III–V colloidal nanocrystals: control of covalent surfaces. Chem. Sci. *11*, 913–922.

48. Park, N., Eagle, F., DeLarme, A., Monahan, M., LoCurto, T., Beck, R., Li, X., and Cossairt, B. (2021). Tuning the Interfacial Stoichiometry of InP Core and InP/ZnSe Core/Shell Quantum Dots.

49. VanOrman, Z.A., Bieber, A.S., Wieghold, S., and Nienhaus, L. (2019). A perspective on triplet fusion upconversion: triplet sensitizers beyond quantum dots. MRS Commun. *9*, 924–935.

50. Huang, Y., Cohen, T.A., Sperry, B.M., Larson, H., Nguyen, H.A., Homer, M.K., Dou, F.Y., Jacoby, L.M., Cossairt, B.M., Gamelin, D.R., et al. (2022). Organic building blocks at inorganic nanomaterial interfaces. Mater. Horiz. *9*, 61–87.

51. Bowers, M.J., McBride, J.R., and Rosenthal, S.J. (2005). White-Light Emission from Magic-Sized Cadmium Selenide Nanocrystals. J. Am. Chem. Soc. *127*, 15378–15379.

52. Dukes, A.D., Schreuder, M.A., Sammons, J.A., McBride, J.R., Smith, N.J., and Rosenthal, S.J. (2008). Pinned emission from ultrasmall cadmium selenide nanocrystals. J. Chem. Phys. *129*, 121102.

53. Bowers II, M.J., McBride, J.R., Garrett, M.D., Sammons, J.A., Dukes III, A.D., Schreuder, M.A., Watt, T.L., Lupini, A.R., Pennycook, S.J., and Rosenthal, S.J. (2009). Structure and Ultrafast Dynamics of White-Light-Emitting CdSe Nanocrystals. J. Am. Chem. Soc. *131*, 5730–5731.

54. VanWie, T., Wysocki, E., McBride, J.R., and Rosenthal, S.J. (2019). Bright Cool White Emission from Ultrasmall CdSe Quantum Dots. Chem. Mater. *31*, 8558–8562.

55. Rosson, T.E., Claiborne, S.M., McBride, J.R., Stratton, B.S., and Rosenthal, S.J. (2012). Bright White Light Emission from Ultrasmall Cadmium Selenide Nanocrystals. J. Am. Chem. Soc. *134*, 8006–8009.

56. Huang, Z., and Lee Tang, M. (2018). Semiconductor Nanocrystal Light Absorbers for Photon Upconversion. J. Phys. Chem. Lett. *9*, 6198–6206.

57. Mahboub, M., Huang, Z., and Tang, M.L. (2016). Efficient Infrared-to-Visible Upconversion with Subsolar Irradiance. Nano Lett. *16*, 7169–7175.

58. Wu, D.M., García-Etxarri, A., Salleo, A., and Dionne, J.A. (2014). Plasmon-Enhanced Upconversion. J. Phys. Chem. Lett. *5*, 4020–4031.

59. VanOrman, Z.A., Bieber, A.S., Wieghold, S., and Nienhaus, L. (2019). A perspective on triplet fusion upconversion: triplet sensitizers beyond quantum dots. MRS Commun. *9*, 924–935.

60. VanOrman, Z.A., Conti, C.R., Strouse, G.F., and Nienhaus, L. (2021). Red-to-Blue Photon Upconversion Enabled by One-Dimensional CdTe Nanorods. Chem. Mater. *33*, 452–458.

61. VanOrman, Z.A., Drozdick, H.K., Wieghold, S., and Nienhaus, L. (2021). Bulk halide perovskites as triplet sensitizers: progress and prospects in photon upconversion. J. Mater. Chem. C *9*, 2685–2694.

62. Gray, V., Xia, P., Huang, Z., Moses, E., Fast, A., A. Fishman, D., I. Vullev, V., Abrahamsson, M., Moth-Poulsen, K., and Tang, M.L. (2017). CdS/ZnS core–shell nanocrystal photosensitizers for visible to UV upconversion. Chem. Sci. *8*, 5488–5496.

63. Xia, P., Schwan, J., Dugger, T.W., Mangolini, L., and Tang, M.L. (2021). Air-Stable Silicon Nanocrystal-Based Photon Upconversion. Adv. Opt. Mater. *9*, 2100453.

64. Wieghold, S., VanOrman, Z.A., and Nienhaus, L. (2021). Halide Perovskites: A Progress Report on Photon Interconversion. Adv. Opt. Mater. *9*, 2001470.

65. Xu, Z., Huang, Z., Jin, T., Lian, T., and Tang, M.L. (2021). Mechanistic Understanding and Rational Design of Quantum Dot/Mediator Interfaces for Efficient Photon Upconversion. Acc. Chem. Res. *54*, 70–80.

66. Huang, Z., Li, X., Yip, B.D., Rubalcava, J.M., Bardeen, C.J., and Tang, M.L. (2015). Nanocrystal Size and Quantum Yield in the Upconversion of Green to Violet Light with CdSe and Anthracene Derivatives. Chem. Mater. *27*, 7503–7507.

67. Rigsby, E.M., Lee, K., Sun, J., Fishman, D.A., and Tang, M.L. (2019). Primary amines enhance triplet energy transfer from both the band edge and trap state from CdSe nanocrystals. J. Chem. Phys. *151*, 174701.

68. Huang, Z., Li, X., Yip, B.D., Rubalcava, J.M., Bardeen, C.J., and Tang, M.L. (2015). Nanocrystal Size and Quantum Yield in the Upconversion of Green to Violet Light with CdSe and Anthracene Derivatives. Chem. Mater. *27*, 7503–7507.

69. Mahboub, M., Xia, P., Van Baren, J., Li, X., Lui, C.H., and Tang, M.L. (2018). Midgap States in PbS Quantum Dots Induced by Cd and Zn Enhance Photon Upconversion. ACS Energy Lett. *3*, 767–772.

70. De Roo, J., Huang, Z., Schuster, N.J., Hamachi, L.S., Congreve, D.N., Xu, Z., Xia, P., Fishman, D.A., Lian, T., Owen, J.S., et al. (2020). Anthracene Diphosphate Ligands for CdSe Quantum Dots; Molecular Design for Efficient Upconversion. Chem. Mater. *32*, 1461–1466.

71. Huang, Z., E. Simpson, D., Mahboub, M., Li, X., and L. Tang, M. (2016). Ligand enhanced upconversion of near-infrared photons with nanocrystal light absorbers. Chem. Sci. *7*, 4101–4104.

72. Mahboub, M., Maghsoudiganjeh, H., Pham, A.M., Huang, Z., and Tang, M.L. (2016). Triplet Energy Transfer from PbS(Se) Nanocrystals to Rubrene: the Relationship between the Upconversion Quantum Yield and Size. Adv. Funct. Mater. *26*, 6091–6097.

73. Toufanian, R., Piryatinski, A., Mahler, A.H., Iyer, R., Hollingsworth, J.A., and Dennis, A.M. (2018). Bandgap Engineering of Indium Phosphide-Based Core/Shell Heterostructures Through Shell Composition and Thickness. Front. Chem. *6*, 567.

74. Saeboe, A.M., Nikiforov, A.Yu., Toufanian, R., Kays, J.C., Chern, M., Casas, J.P., Han, K., Piryatinski, A., Jones, D., and Dennis, A.M. (2021). Extending the Near-Infrared Emission Range of Indium Phosphide Quantum Dots for Multiplexed In Vivo Imaging. Nano Lett. *21*, 3271–3279.

75. Kim, K., Lee, H., Ahn, J., and Jeong, S. (2012). Highly luminescing multi-shell semiconductor nanocrystals InP/ZnSe/ZnS. Appl. Phys. Lett. *101*, 073107.

76. Friedfeld, M.R., Stein, J.L., Johnson, D.A., Park, N., Henry, N.A., Enright, M.J., Mocatta, D., and Cossairt, B.M. (2019). Effects of Zn2+ and Ga3+ doping on the quantum yield of cluster-derived InP quantum dots. J. Chem. Phys. *151*, 194702.

77. Kim, Y., Ham, S., Jang, H., Min, J.H., Chung, H., Lee, J., Kim, D., and Jang, E. (2019). Bright and Uniform Green Light Emitting InP/ZnSe/ZnS Quantum Dots for Wide Color Gamut Displays. ACS Appl. Nano Mater. *2*, 1496–1504.

78. Kim, K., Yoo, D., Choi, H., Tamang, S., Ko, J.-H., Kim, S., Kim, Y.-H., and Jeong, S. (2016). Halide–Amine Co-Passivated Indium Phosphide Colloidal Quantum Dots in Tetrahedral Shape. Angew. Chem. Int. Ed. *55*, 3714–3718.

79. Stein, J.L., Mader, E.A., and Cossairt, B.M. (2016). Luminescent InP Quantum Dots with Tunable Emission by Post-Synthetic Modification with Lewis Acids. J. Phys. Chem. Lett. *7*, 1315–1320.

80. Gary, D.C., Terban, M.W., Billinge, S.J.L., and Cossairt, B.M. (2015). Two-Step Nucleation and Growth of InP Quantum Dots via Magic-Sized Cluster Intermediates. Chem. Mater. *27*, 1432–1441.

81. Gary, D.C., and Cossairt, B.M. (2013). Role of Acid in Precursor Conversion During InP Quantum Dot Synthesis. Chem. Mater. *25*, 2463–2469.

82. Friedfeld, M.R., Johnson, D.A., and Cossairt, B.M. (2019). Conversion of InP Clusters to Quantum Dots. Inorg. Chem. *58*, 803–810.

83. Won, Y.-H., Cho, O., Kim, T., Chung, D.-Y., Kim, T., Chung, H., Jang, H., Lee, J., Kim, D., and Jang, E. (2019). Highly efficient and stable InP/ZnSe/ZnS quantum dot light-emitting diodes. Nature *575*, 634–638.

84. Toufanian, R., Chern, M., Kong, V.H., and Dennis, A.M. (2021). Engineering Brightness-Matched Indium Phosphide Quantum Dots. Chem. Mater. *33*, 1964–1975.

85. Yarema, O., Yarema, M., Bozyigit, D., Lin, W.M.M., and Wood, V. (2015). Independent Composition and Size Control for Highly Luminescent Indium-Rich Silver Indium Selenide Nanocrystals. ACS Nano *9*, 11134–11142.

86. Yarema, O., Bozyigit, D., Rousseau, I., Nowack, L., Yarema, M., Heiss, W., and Wood, V. (2013). Highly Luminescent, Size- and Shape-Tunable Copper Indium Selenide Based Colloidal Nanocrystals. Chem. Mater. *25*, 3753–3757.

87. He, C., Weinberg, D.J., Nepomnyashchii, A.B., Lian, S., and Weiss, E.A. (2016). Control of the Redox Activity of PbS Quantum Dots by Tuning Electrostatic Interactions at the Quantum Dot/Solvent Interface. J. Am. Chem. Soc. *138*, 8847–8854.

88. Chen, S., Thota, S., Singh, G., Aímola, T.J., Koenigsmann, C., and Zhao, J. (2017). Synthesis of hollow Pt–Ag nanoparticles by oxygen-assisted acid etching as electrocatalysts for the oxygen reduction reaction. RSC Adv. *7*, 46916–46924.

89. Ung, D., and Cossairt, B.M. (2019). Effect of Surface Ligands on CoP for the Hydrogen Evolution Reaction. ACS Appl. Energy Mater. *2*, 1642–1645.

90. Lian, S., Kodaimati, M.S., and Weiss, E.A. (2018). Photocatalytically Active Superstructures of Quantum Dots and Iron Porphyrins for Reduction of CO2 to CO in Water. ACS Nano *12*, 568–575.

91. Arcudi, F., Đorđević, L., Nagasing, B., Stupp, S.I., and Weiss, E.A. (2021). Quantum Dot-Sensitized Photoreduction of CO2 in Water with Turnover Number > 80,000. J. Am. Chem. Soc. *143*, 18131–18138.

92. Yadav, V., Lowe, J.S., Shumski, A.J., Liu, E.Z., Greeley, J., and Li, C.W. (2020). Modulating the Structure and Hydrogen Evolution Reactivity of Metal Chalcogenide Complexes through Ligand Exchange onto Colloidal Au Nanoparticles. ACS Catal. *10*, 13305–13313.

93. Kodaimati, M.S., Lian, S., Schatz, G.C., and Weiss, E.A. (2018). Energy transfer-enhanced photocatalytic reduction of protons within quantum dot light-harvesting–catalyst assemblies. Proc. Natl. Acad. Sci. *115*, 8290–8295.

94. Carlton, C.E., Chen, S., Ferreira, P.J., Allard, L.F., and Shao-Horn, Y. (2012). Sub-Nanometer-Resolution Elemental Mapping of “Pt3Co” Nanoparticle Catalyst Degradation in Proton-Exchange Membrane Fuel Cells. J. Phys. Chem. Lett. *3*, 161–166.

95. Huang, X., Shumski, A.J., Zhang, X., and Li, C.W. (2018). Systematic Control of Redox Properties and Oxygen Reduction Reactivity through Colloidal Ligand-Exchange Deposition of Pd on Au. J. Am. Chem. Soc. *140*, 8918–8923.

96. Chen, S., Ferreira, P.J., Sheng, W., Yabuuchi, N., Allard, L.F., and Shao-Horn, Y. (2008). Enhanced Activity for Oxygen Reduction Reaction on "Pt3Co" Nanoparticles: Direct Evidence of Percolated and Sandwich-Segregation Structures. J. Am. Chem. Soc. *130*, 13818–13819.

97. Chen, S., Sheng, W., Yabuuchi, N., Ferreira, P.J., Allard, L.F., and Shao-Horn, Y. (2009). Origin of Oxygen Reduction Reaction Activity on "Pt3Co" Nanoparticles: Atomically Resolved Chemical Compositions and Structures. J. Phys. Chem. C *113*, 1109–1125.

98. McClelland, K.P., and Weiss, E.A. (2019). Selective Photocatalytic Oxidation of Benzyl Alcohol to Benzaldehyde or C–C Coupled Products by Visible-Light-Absorbing Quantum Dots. ACS Appl. Energy Mater. *2*, 92–96.

99. Zhang, Z., Rogers, C.R., and Weiss, E.A. (2020). Energy Transfer from CdS QDs to a Photogenerated Pd Complex Enhances the Rate and Selectivity of a Pd-Photocatalyzed Heck Reaction. J. Am. Chem. Soc. *142*, 495–501.

100. McClelland, K.P., Clemons, T.D., Stupp, S.I., and Weiss, E.A. (2020). Semiconductor Quantum Dots Are Efficient and Recyclable Photocatalysts for Aqueous PET-RAFT Polymerization. ACS Macro Lett. *9*, 7–13.

101. Lal, S., Clare, S.E., and Halas, N.J. (2008). Nanoshell-Enabled Photothermal Cancer Therapy: Impending Clinical Impact. Acc. Chem. Res. *41*, 1842–1851.

102. West, J.L., and Halas, N.J. (2003). Engineered Nanomaterials for Biophotonics Applications: Improving Sensing, Imaging, and Therapeutics. Annu. Rev. Biomed. Eng. *5*, 285–292.

103. Alkilany, A.M., Thompson, L.B., Boulos, S.P., Sisco, P.N., and Murphy, C.J. (2012). Gold nanorods: Their potential for photothermal therapeutics and drug delivery, tempered by the complexity of their biological interactions. Adv. Drug Deliv. Rev. *64*, 190–199.

104. Gobin, A.M., Lee, M.H., Halas, N.J., James, W.D., Drezek, R.A., and West, J.L. (2007). Near-Infrared Resonant Nanoshells for Combined Optical Imaging and Photothermal Cancer Therapy. Nano Lett. *7*, 1929–1934.

105. Hirsch, L.R., Stafford, R.J., Bankson, J.A., Sershen, S.R., Rivera, B., Price, R.E., Hazle, J.D., Halas, N.J., and West, J.L. (2003). Nanoshell-mediated near-infrared thermal therapy of tumors under magnetic resonance guidance. Proc. Natl. Acad. Sci. *100*, 13549–13554.

106. Scholl, J.A., Koh, A.L., and Dionne, J.A. (2012). Quantum plasmon resonances of individual metallic nanoparticles. Nature *483*, 421–427.

107. Halas, N. (2005). Playing with Plasmons: Tuning the Optical Resonant Properties of Metallic Nanoshells. MRS Bull. *30*, 362–367.

108. Grzincic, E.M., and Murphy, C.J. (2015). Gold Nanorods Indirectly Promote Migration of Metastatic Human Breast Cancer Cells in Three-Dimensional Cultures. ACS Nano *9*, 6801–6816.

109. Cole, J.R., Mirin, N.A., Knight, M.W., Goodrich, G.P., and Halas, N.J. (2009). Photothermal Efficiencies of Nanoshells and Nanorods for Clinical Therapeutic Applications. J. Phys. Chem. C *113*, 12090–12094.

110. Bardhan, R., Lal, S., Joshi, A., and Halas, N.J. (2011). Theranostic Nanoshells: From Probe Design to Imaging and Treatment of Cancer. Acc. Chem. Res. *44*, 936–946.

111. O'Neal, D.P., Hirsch, L.R., Halas, N.J., Payne, J.D., and West, J.L. (2004). Photo-thermal tumor ablation in mice using near infrared-absorbing nanoparticles. Cancer Lett. *209*, 171–176.

112. Zhang, X., Falagan-Lotsch, P., and Murphy, C.J. (2021). Nanoparticles Interfere with Chemotaxis: An Example of Nanoparticles as Molecular "Knockouts" at the Cellular Level. ACS Nano *15*, 8813–8825.

113. Bardhan, R., Grady, N.K., Cole, J.R., Joshi, A., and Halas, N.J. (2009). Fluorescence Enhancement by Au Nanostructures: Nanoshells and Nanorods. ACS Nano *3*, 744–752.

114. West, J.L., and Halas, N.J. (2000). Applications of nanotechnology to biotechnology: Commentary. Curr. Opin. Biotechnol. *11*, 215–217.

115. Murphy, C.J., Gole, A.M., Stone, J.W., Sisco, P.N., Alkilany, A.M., Goldsmith, E.C., and Baxter, S.C. (2008). Gold Nanoparticles in Biology: Beyond Toxicity to Cellular Imaging. Acc. Chem. Res. *41*, 1721–1730.

116. Kovtun, O., Tomlinson, I.D., Sakrikar, D.S., Chang, J.C., Blakely, R.D., and Rosenthal, S.J. (2011). Visualization of the Cocaine-Sensitive Dopamine Transporter with Ligand-Conjugated Quantum Dots. ACS Chem. Neurosci. *2*, 370–378.

117. Boulos, S.P., Prigozhin, M.B., Liu, Y., Wirth, A.J., Boppart, S.A., Gruebele, M., and Murphy, C.J. (2013). The Gold Nanorod-Biology Interface: From Proteins to Cells to Tissue. Curr. Phys. Chem. *3*, 1–8.

118. Marbella, L.E., Andolina, C.M., Smith, A.M., Hartmann, M.J., Dewar, A.C., Johnston, K.A., Daly, O.H., and Millstone, J.E. (2014). Gold-Cobalt Nanoparticle Alloys Exhibiting Tunable Compositions, Near-Infrared Emission, and High T2 Relaxivity. Adv. Funct. Mater. *24*, 6532–6539.

119. Andolina, C.M., Dewar, A.C., Smith, A.M., Marbella, L.E., Hartmann, M.J., and Millstone, J.E. (2013). Photoluminescent Gold–Copper Nanoparticle Alloys with Composition-Tunable Near-Infrared Emission. J. Am. Chem. Soc. *135*, 5266–5269.

120. Loo, C., Hirsch, L., Lee, M.-H., Chang, E., West, J., Halas, N., and Drezek, R. (2005). Gold nanoshell bioconjugates for molecular imaging in living cells. Opt. Lett. *30*, 1012–1014.

121. Huschka, R., Neumann, O., Barhoumi, A., and Halas, N.J. (2010). Visualizing Light-Triggered Release of Molecules Inside Living Cells. Nano Lett. *10*, 4117–4122.

122. Sershen, S.R., Westcott, S.L., Halas, N.J., and West, J.L. (2000). Temperature-sensitive polymer–nanoshell composites for photothermally modulated drug delivery. J. Biomed. Mater. Res. *51*, 293–298.

123. Huschka, R., Zuloaga, J., Knight, M.W., Brown, L.V., Nordlander, P., and Halas, N.J. (2011). Light-Induced Release of DNA from Gold Nanoparticles: Nanoshells and Nanorods. J. Am. Chem. Soc. *133*, 12247–12255.

124. Lowery, A.R., Gobin, A.M., Day, E.S., Halas, N.J., and West, J.L. (2006). Immunonanoshells for targeted photothermal ablation of tumor cells. Int. J. Nanomedicine *1*, 149–154.

125. Barhoumi, A., Huschka, R., Bardhan, R., Knight, M.W., and Halas, N.J. (2009). Light-induced release of DNA from plasmon-resonant nanoparticles: Towards light-controlled gene therapy. Chem. Phys. Lett. *482*, 171–179.

126. Sisco, P.N., Wilson, C.G., Chernak, D., Clark, J.C., Grzincic, E.M., Ako-Asare, K., Goldsmith, E.C., and Murphy, C.J. (2014). Adsorption of Cellular Proteins to Polyelectrolyte-Functionalized Gold Nanorods: A Mechanism for Nanoparticle Regulation of Cell Phenotype? PLOS ONE *9*, e86670.

127. Bardhan, R., Chen, W., Perez-Torres, C., Bartels, M., Huschka, R.M., Zhao, L.L., Morosan, E., Pautler, R.G., Joshi, A., and Halas, N.J. (2009). Nanoshells with Targeted Simultaneous Enhancement of Magnetic and Optical Imaging and Photothermal Therapeutic Response. Adv. Funct. Mater. *19*, 3901–3909.

128. Andolina, C.M., Crawford, S.E., Smith, A.M., Johnston, K.A., Straney, P.J., Marbella, L.E., Tolman, N.L., Hochuli, T.J., and Millstone, J.E. (2018). Near-Infrared Photoluminescence from Small Copper, Silver, and Gold Nanoparticles. ChemNanoMat *4*, 265–268.

129. Crawford, S.E., Hartmann, M.J., and Millstone, J.E. (2019). Surface Chemistry-Mediated Near-Infrared Emission of Small Coinage Metal Nanoparticles. Acc. Chem. Res. *52*, 695–703.

130. Stone, J.W., Sisco, P.N., Goldsmith, E.C., Baxter, S.C., and Murphy, C.J. (2007). Using Gold Nanorods to Probe Cell-Induced Collagen Deformation. Nano Lett. *7*, 116–119.

131. Wilson, C.G., Sisco, P.N., Goldsmith, E.C., and Murphy, C.J. (2009). Glycosaminoglycan-functionalized gold nanorods: interactions with cardiac cells and type I collagen. J. Mater. Chem. *19*, 6332–6340.

132. Alkilany, A.M., Boulos, S.P., Lohse, S.E., Thompson, L.B., and Murphy, C.J. (2014). Homing Peptide-Conjugated Gold Nanorods: The Effect of Amino Acid Sequence Display on Nanorod Uptake and Cellular Proliferation. Bioconjug. Chem. *25*, 1162–1171.

133. Falagan-Lotsch, P., Grzincic, E.M., and Murphy, C.J. (2016). One low-dose exposure of gold nanoparticles induces long-term changes in human cells. Proc. Natl. Acad. Sci. *113*, 13318–13323.

134. Alkilany, A.M., Lohse, S.E., and Murphy, C.J. (2013). The Gold Standard: Gold Nanoparticle Libraries To Understand the Nano–Bio Interface. Acc. Chem. Res. *46*, 650–661.

135. Zhang, D., Neumann, O., Wang, H., Yuwono, V.M., Barhoumi, A., Perham, M., Hartgerink, J.D., Wittung-Stafshede, P., and Halas, N.J. (2009). Gold Nanoparticles Can Induce the Formation of Protein-based Aggregates at Physiological pH. Nano Lett. *9*, 666–671.

136. Grzincic, E.M., Yang, J.A., Drnevich, J., Falagan-Lotsch, P., and Murphy, C.J. (2015). Global Transcriptomic Analysis of Model Human Cell Lines Exposed to Surface-Modified Gold Nanoparticles: The Effect of Surface Chemistry. Nanoscale *7*, 1349–1362.

137. Park, J., Jayaraman, A., Schrader, A.W., Hwang, G.W., and Han, H.-S. (2020). Controllable modulation of precursor reactivity using chemical additives for systematic synthesis of high-quality quantum dots. Nat. Commun. *11*, 5748.

Figures

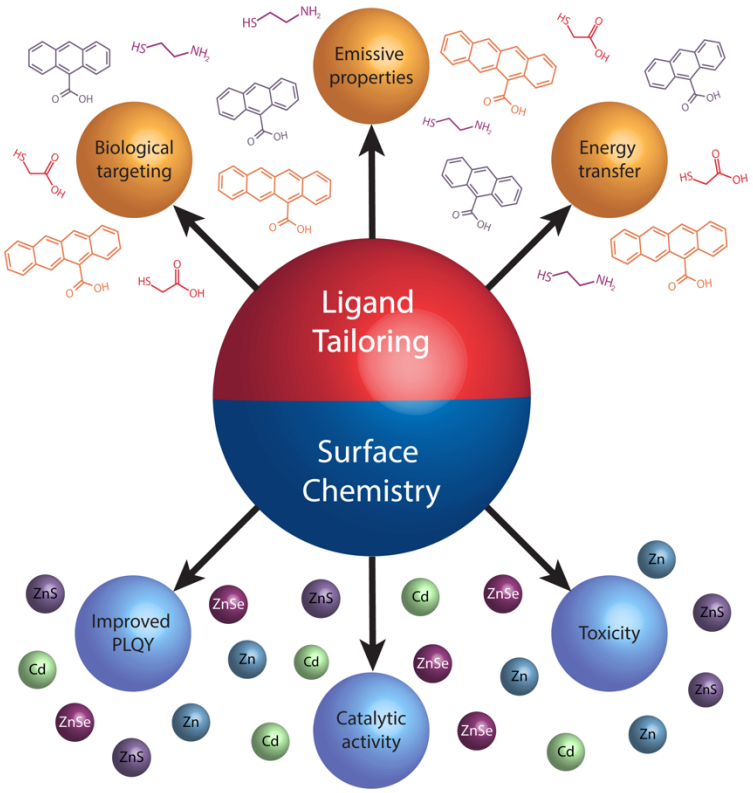

Figure 1. Overview schematic highlighting the tunability of the NC/NP properties by ligand tailoring enabling biological targeting, tuning of the emissive properties, or enabling or retarding energy transfer. Alteration of the NC surface chemistry can lead to improved PLQYs, changes in the catalytic activity and NC/NP toxicity.

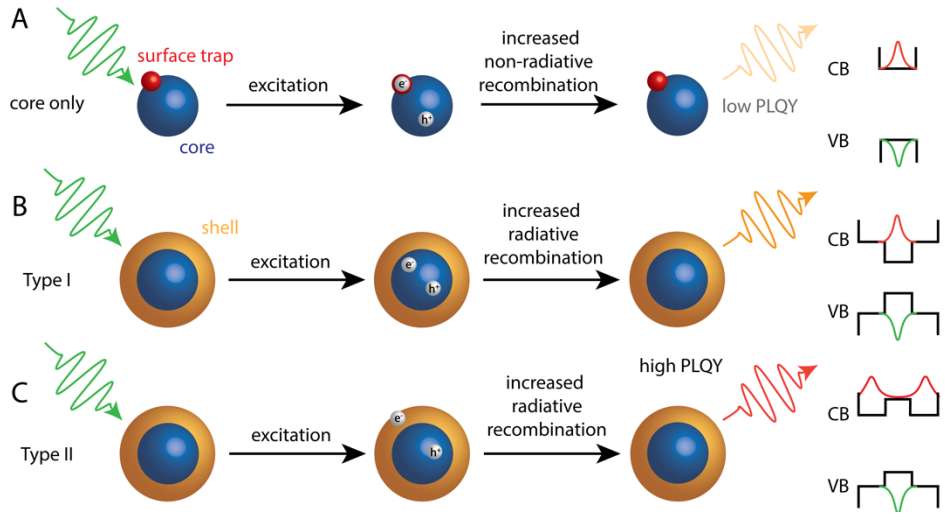

Figure 2. Illustration of the impact of shelling on the excitonic properties of the NC.

A. Schematic of the effect of surface trap states on the PLQY of a NC. Trapping into surface trap states increases nonradiative decay of the exciton. The localization of the electron (red) and hole (green) wavefunction for a core-only NC is shown on the right.
B. Type I core/shell NCs. The shell passivates the surface trap states, improving the PLQY from a core-only NC and can result in a slight red shift of the PL. The band alignment in a type I core/shell NC, shown on the right, confines both electron and hole to the core.
C. Type II core/shell NCs. The band alignment causes electron delocalization into the shell while the hole remains localized in the core. The reduced exciton confinement results in redshifted emission.

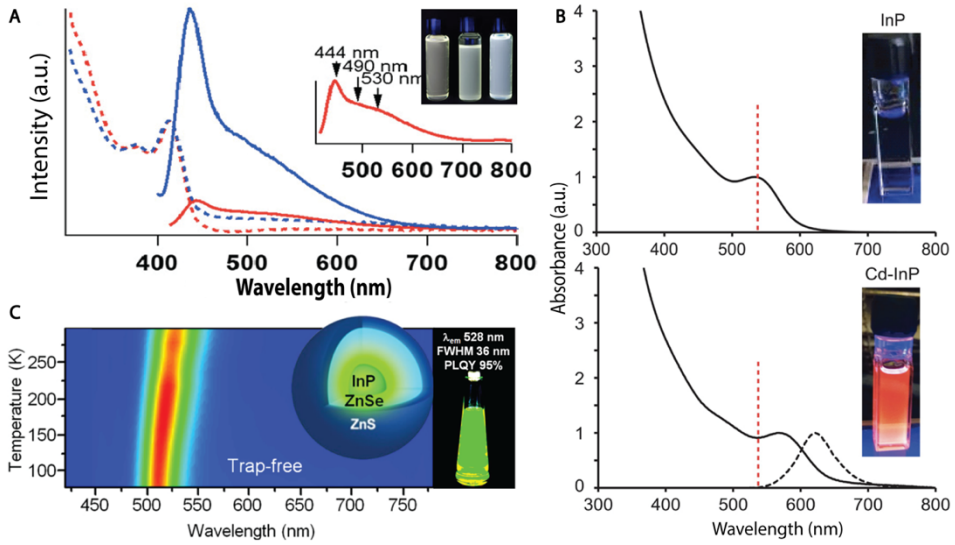

Figure 3. Optical properties of semiconductor NCs based on ligand and surface treatments.

A. Absorption (dashed) and emission (solid) spectra of CdSe NCs both untreated (red) and treated (blue) with citric acid. The inset highlights three emission features in the emission spectra of untreated CdSe which contribute to white light emission. The photo shows the following samples under UV excitation (from left to right) untreated NCs, formic acid treated NCs, and citric acid treated NCs. Adapted from *Chem. Mater.* 2019, 31, 20, 8558–8562. Copyright 2019 American Chemical Society.

B. Absorption spectra of untreated InP NCs (top). The red dashed line indicates the wavelength of the lowest energy absorption feature in untreated InP NCs. Absorption (solid) and emission (dashed) of and InP NCs after post-synthetic addition of cadmium (bottom). There is a distinct red shift in absorption after the addition of cadmium. Reprinted with permission from *J. Phys. Chem. Lett.* 2016, 7, 7, 1315–1320. Copyright 2016 American Chemical Society.

C. Temperature-dependent emission of InP/ZnSe/ZnS core/shell/shell NCs. A small red shift in emission wavelength is observed with increasing temperature. A schematic of the structure of the InP/ZnSe/ZnS core/shell/shell NC is shown as an inset. On the right is a photo of the green emitting InP/ZnSe/ZnS core/shell/shell NCs under 430 nm illumination. Adapted from *ACS Appl. Nano Mater.* 2019, 2, 3, 1496–1504. Copyright 2019 American Chemical Society.

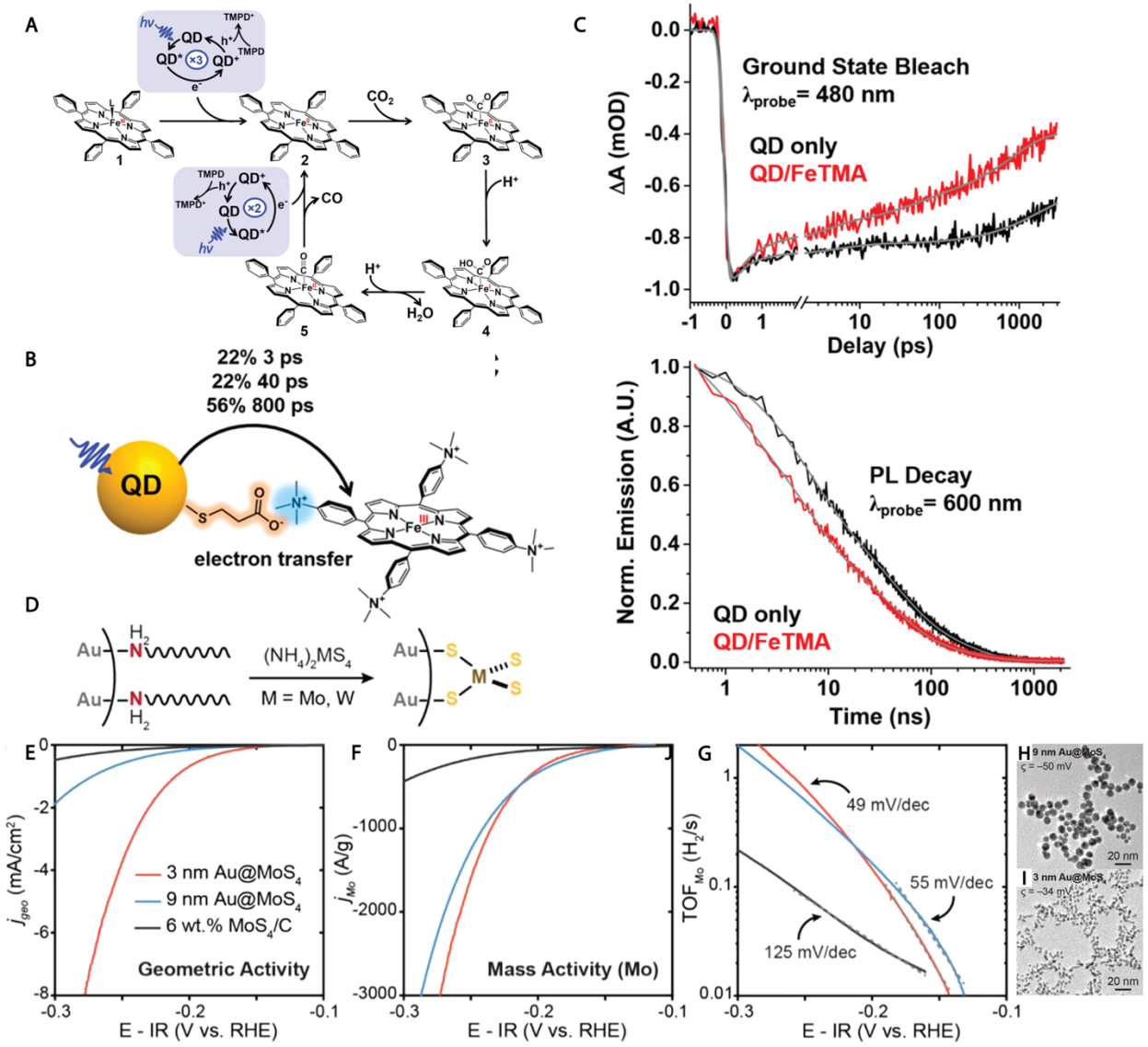

Figure 4. Catalytic behavior of NC-based systems.

A. Mechanism of $CuInS_2$ sensitized CO_2 reduction using a FeTPP catalyst. Adapted with permission from *J. Am. Chem. Soc.* 2017, 139, 26, 8931–8938. Copyright 2017 American Chemical Society.

B. Diagram of electron sensitization of FeTMA using a QD, illustrating photosensitization. The quantum dot absorbs incident light, and the resulting excited electron undergoes an electron transfer to FeTMA which can then catalytically reduce CO_2 to CO. Adapted with permission from *ACS Nano* 2018, 12, 1, 568–575. Copyright 2018 American Chemical Society.

C. Transient absorption kinetics probed at 480 nm (top) and PL decays probed at 600 nm under 450 nm excitation (bottom) of MPA-capped QDs plain(black) and with FeTMA added (red; adjusted by 1.2 to account for FeTMA absorption). Adapted with permission from *ACS Nano* 2018, 12, 1, 568–575. Copyright 2018 American Chemical Society.

D. Colloidal ligand-exchange reaction scheme between AuNP coated with oleylamine and metallic chalcogenide complexes. The AuNP undergoes a ligand exchange resulting in MS_4 complexed to its surface, in the place of the native oleylamine ligands. Reprinted with permission from *ACS Catal.* 2020, 10, 22, 13305–13313. Copyright 2020 American Chemical Society.
E. Activity of MoS_4 treated AuNPs with 3 nm diameter (red) and 9nm diameter (blue), as well as a 6% $(NH_4)_2MoS_4$ adsorbed to glassy carbon as a control (black). This figure displays the geometric activity of each, demonstrating that the 3 nm AuNP has the highest geometric activity. Adapted with permission from *ACS Catal.* 2020, 10, 22, 13305–13313. Copyright 2020 American Chemical Society.
F. Mass Activity of MoS_4 treated AuNPs with 3 nm diameter (red) and 9nm diameter (blue), as well as a 6% $(NH_4)_2MoS_4$ adsorbed to glassy carbon as a control (black). To find mass activity, the geometric activity was normalized to the mass of the appropriate sample. The two AuNPs exhibit comparable mass activity, making the 3 nm AuNPs a superior option as they require less material. Adapted with permission from *ACS Catal.* 2020, 10, 22, 13305–13313. Copyright 2020 American Chemical Society.
G. TOF of MoS_4 treated AuNPs with 3 nm diameter (red) and 9 nm diameter (blue), as well as a 6% $(NH_4)_2MoS_4$ adsorbed to glassy carbon as a control (black). While these samples exhibit TOF below the recorded record value, the increased performance of AuNPs over the carbon control indicate the importance of functionalization on the performance of MoS_4 as a catalyst. Adapted with permission from *ACS Catal.* 2020, 10, 22, 13305–13313. Copyright 2020 American Chemical Society.
H. TEM image of 9 nm AuNP after MoS_4 exchange. Reprinted with permission from *ACS Catal.* 2020, 10, 22, 13305–13313. Copyright 2020 American Chemical Society.
I. TEM image of 3 nm AuNP after MoS_4 exchange. Reprinted with permission from *ACS Catal.* 2020, 10, 22, 13305–13313. Copyright 2020 American Chemical Society.

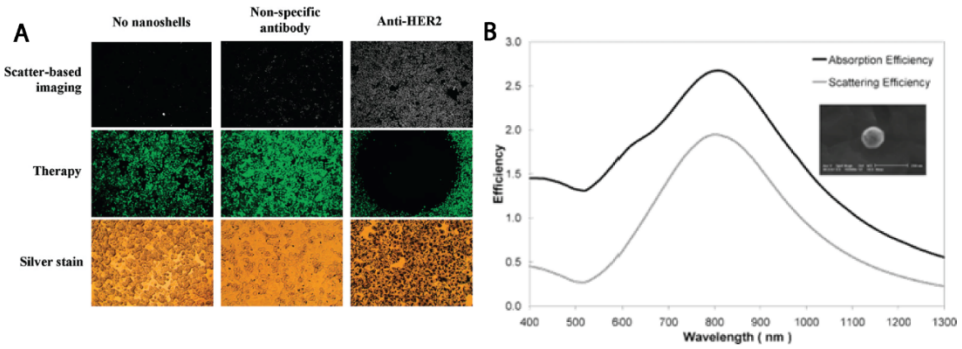

Figure 5. Use of NIR absorbing NP in cancer treatment.

A. Effects of laser therapy on HER2 positive SKBr3 breast cancer cells treated with no NPs (left), NPs treated with a non-specific antibody that would not target the cells shown (middle), and NPs with Anti-HER2 antibodies (right). Images collected using scatter-based darkfield imaging (top) display the expression of HER2, as the targeted NPs display increased scattering visible as a lighter image compared to a control and non-specific NPs. Calcein fluorescent staining after irradiation with 820 nm laser (middle) displays cell death, visible in the black region, only where the laser hit the cells treated with the Anti-HER NPs. Imaging using a silver stain (bottom) indicates that only the Anti-HER NPs significantly bind to cells, where the NP are indicated by dark spots in the image. Reprinted with permission from *Nano Lett.* 2005, 5, 4, 709–711. Copyright 2005 American Chemical Society.
B. NIR scattering (grey), and absorption (black) efficiencies of NPs used for SKBr3 breast cancer treatment. The inset is an SEM image of a NP with a 140nm diameter, scale bar: 200nm. The NP structure is a 120nm silica NP with a 10nm thick shell of gold colloid. Reprinted with permission from *Nano Lett.* 2005, 5, 4, 709–711. Copyright 2005 American Chemical Society.

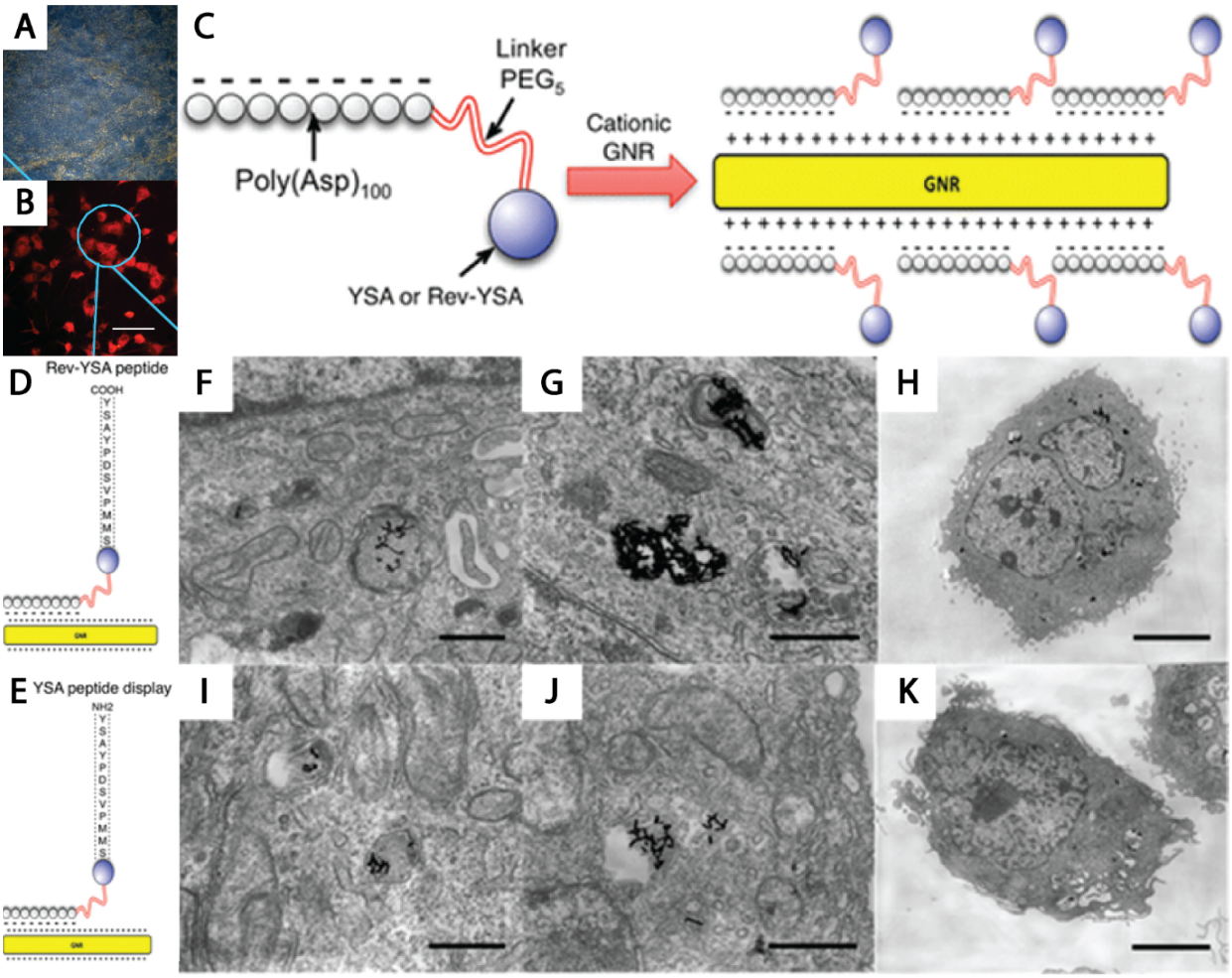

Figure 6. Biological uses of NIR/IR absorbing NPs.

A. Dark field optical spectroscopy of neonatal cardiac fibroblasts treated with AuNPs. The AuNPs are visible as the yellow spots due to scattering. Reprinted with permission from *Acc. Chem. Res.* 2008, 41, 12, 1721–1730. Copyright 2008 American Chemical Society.
B. Fluorescent imaging of neonatal cardiac fibroblasts treated with AuNPs and stained with a fluorescent dye. Reprinted with permission from *Acc. Chem. Res.* 2008, 41, 12, 1721–1730. Copyright 2008 American Chemical Society.
C. Schematic illustrating the modification of the CTAB coated gold nanorods (GNRs) with YSA-PEG-poly(Asp) ligand. The ligand is attached *via* a layer-by-layer procedure. Reprinted with permission from *Bioconjugate Chem.* 2014, 25, 6, 1162–1171. Copyright 2014 American Chemical Society.
D. Peptide arrangement of a EphA2 homing peptide, YSA-peptide on the AuNR surface. Reprinted with permission from *Bioconjugate Chem.* 2014, 25, 6, 1162–1171. Copyright 2014 American Chemical Society.
E. Peptide arrangement of the reverse YSA-peptide (Rev-YSA) on the AuNR surface. Reprinted with permission from *Bioconjugate Chem.* 2014, 25, 6, 1162–1171. Copyright 2014 American Chemical Society.

F. TEM image of PC3 cells incubated with YSA AuNRs for two hours. The black spots indicate AuNR in the cells. YSA AuNR exhibit higher concentrations of AuNRs than Rev-YSA AuNRs. The higher amount of AuNR (visible as black spots) in these cells compared to those treated with Rev-YSA AuNRs indicates the YSA AuNRs are better taken up by cells. Scale bar: 1 μM. Reprinted with permission from *Bioconjugate Chem.* 2014, 25, 6, 1162–1171. Copyright 2014 American Chemical Society.
G. TEM image of PC3 cells incubated with YSA AuNRs for 24 hours. Scale bar: 0.5 μM. The higher amount of AuNR (visible as black spots) in these cells compared to those treated with Rev-YSA AuNRs indicates the YSA AuNRs are better taken up by cells. Reprinted with permission from *Bioconjugate Chem.* 2014, 25, 6, 1162–1171. Copyright 2014 American Chemical Society.
H. TEM image of PC3 cells incubated with YSA AuNRs for 24 hours. Scale bar: 5 μM. The higher amount of AuNR (visible as black spots) in these cells compared to those treated with Rev-YSA AuNRs indicates the YSA AuNRs are better taken up by cells. Reprinted with permission from *Bioconjugate Chem.* 2014, 25, 6, 1162–1171. Copyright 2014 American Chemical Society.
I. TEM image of PC3 cells incubated with 0.1 nM Rev-YSA AuNRs for 2 hours. Scale bar: 0.5 μM. Reprinted with permission from *Bioconjugate Chem.* 2014, 25, 6, 1162–1171. Copyright 2014 American Chemical Society.
J. TEM image of PC3 cells incubated with Rev-YSA AuNRs for 24 hours. Scale bar: 0.5 μM. Reprinted with permission from *Bioconjugate Chem.* 2014, 25, 6, 1162–1171. Copyright 2014 American Chemical Society.
K. TEM image of PC3 cells incubated with Rev-YSA AuNRs for 24 hours. Scale bar: 5 μM. Reprinted with permission from *Bioconjugate Chem.* 2014, 25, 6, 1162–1171. Copyright 2014 American Chemical Society.